Spectral Hardening Reveals Afterglow Emergence: A Case Study of GRB 250404A/EP250404a

arXiv: 2506.00435

Yi-Han Iris Yin
Nanjing University

Collaborators: NJU Bin-Bin Zhang GRB Team, EP DS+TA, Mephisto Team, TNOT Team, NAOC Xu Dong Team, SYSU 80cm Team, GMG-2.4m Team, Schmidt Team, BOOTES Team, HUST Weihua Lei Team, Bing Zhang, et al.

Challenges of tracing the GRB prompt emission-afterglow transition

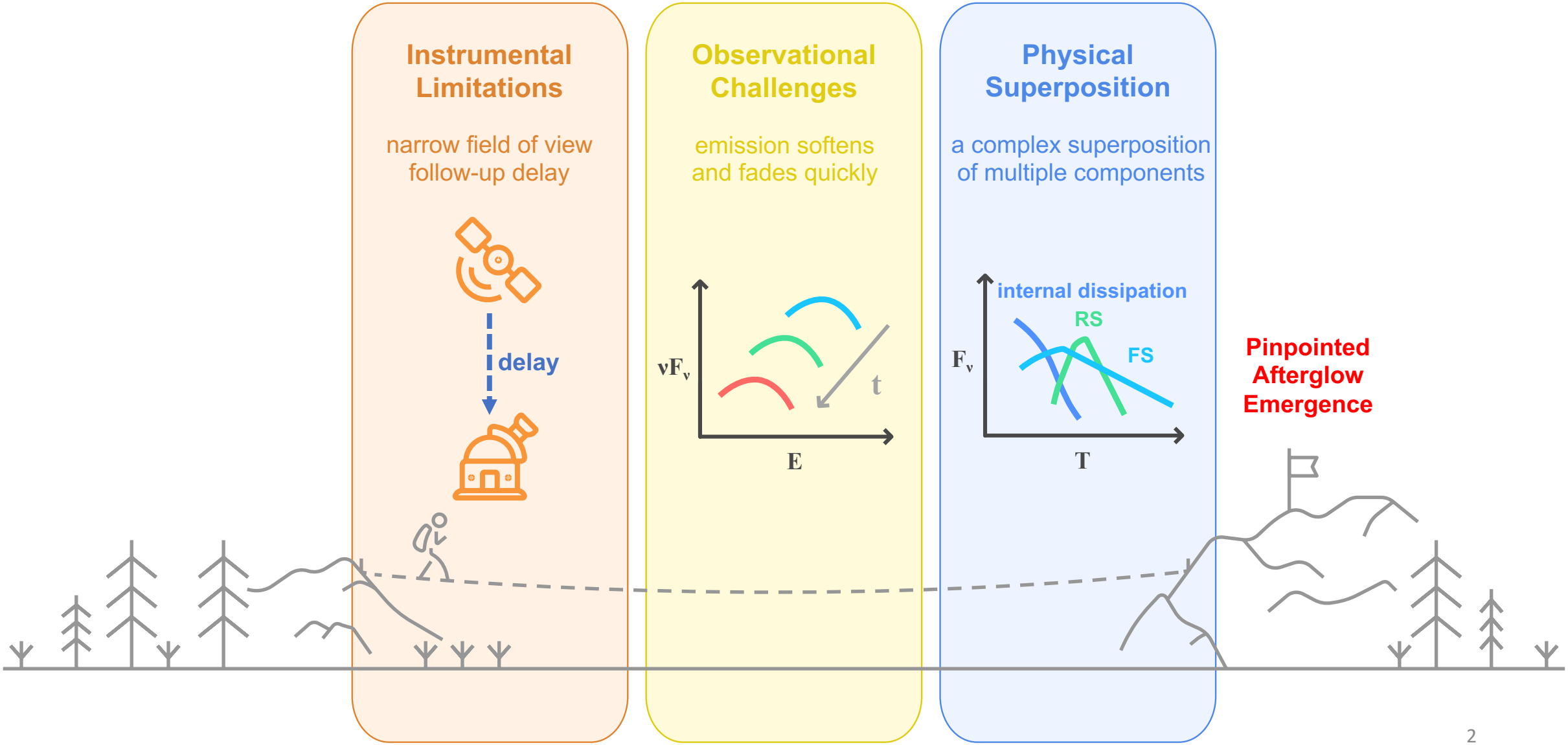

Challenges of tracing the GRB prompt emission-afterglow transition

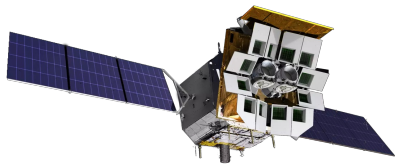

Wide FOV EP/WXT and automatic follow-up system with EP/FXT

capturing long-duration GRB emission in X-rays

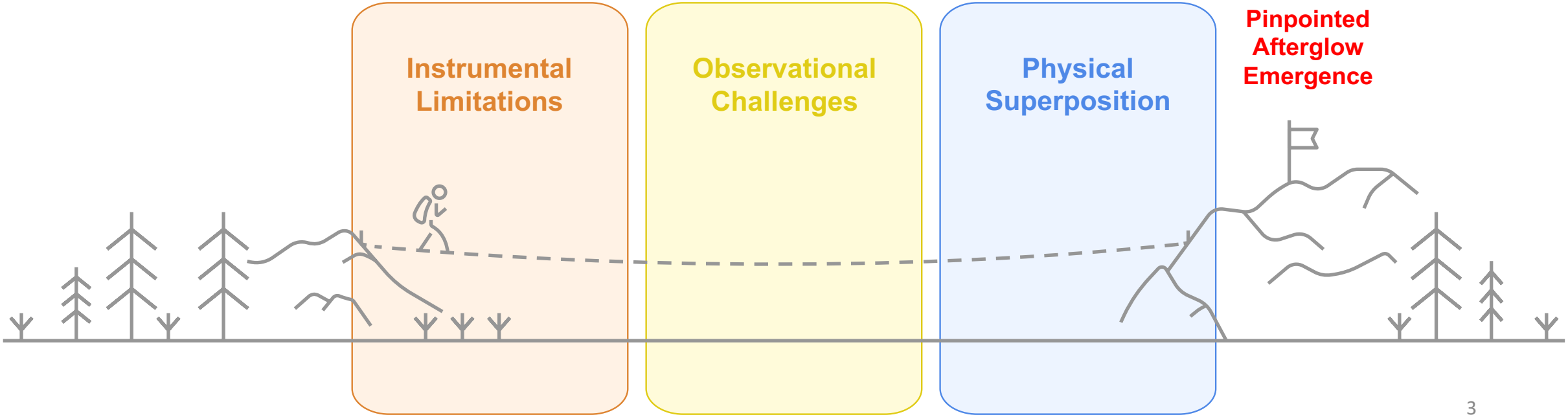

Content

- EP and GBM detections of GRB 250404A/EP250404a
- Spectral fitting
- Spectral evolution and transition signature
- Multiwavelength observation and afterglow fitting
- Discussion
- Summary

EP250404a detections

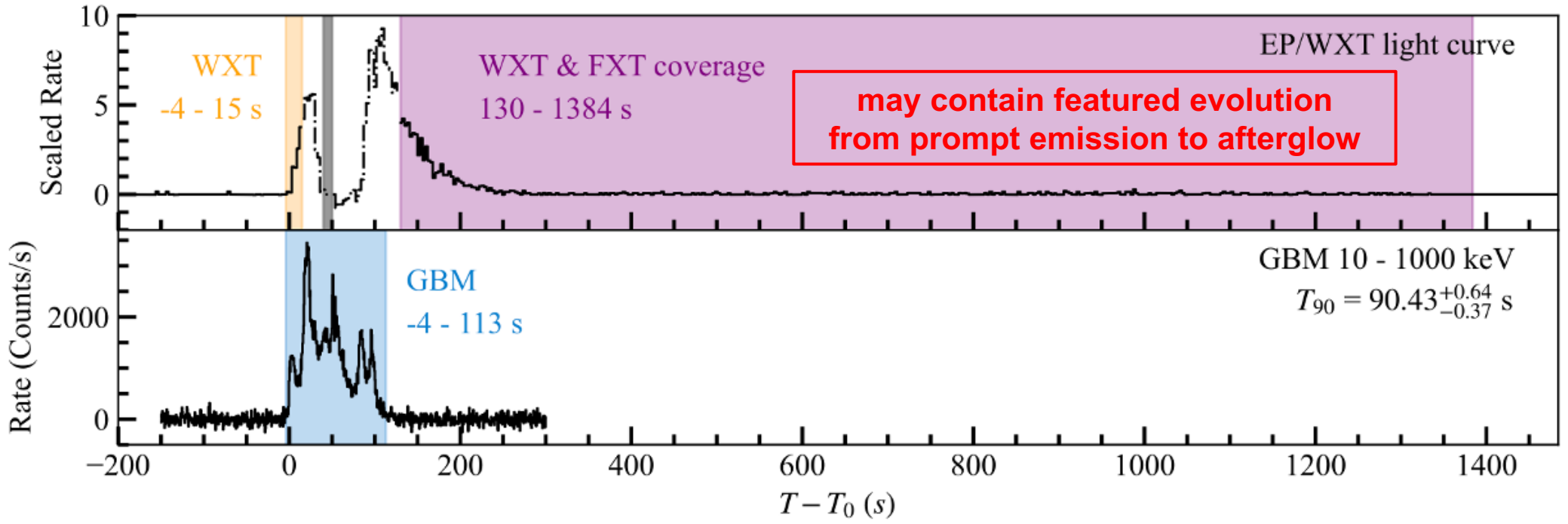

EP and GBM detections of GRB 250404A/EP250404a

- Triggered by Fermi/GBM and EP/WXT at 2025-04-04T14:19:46 (T_0)
- T_{90} = 90.43 s (10–1000 keV)
- WXT coverage T_0 + [-4, 15] s
- FXT automatic follow-up coverage T_0 + [130, 1384] s
- X-ray dust scattering feature within T_0 + [4324, 7143] s (Yong Chen's talk)

EP250404a spectral fittings

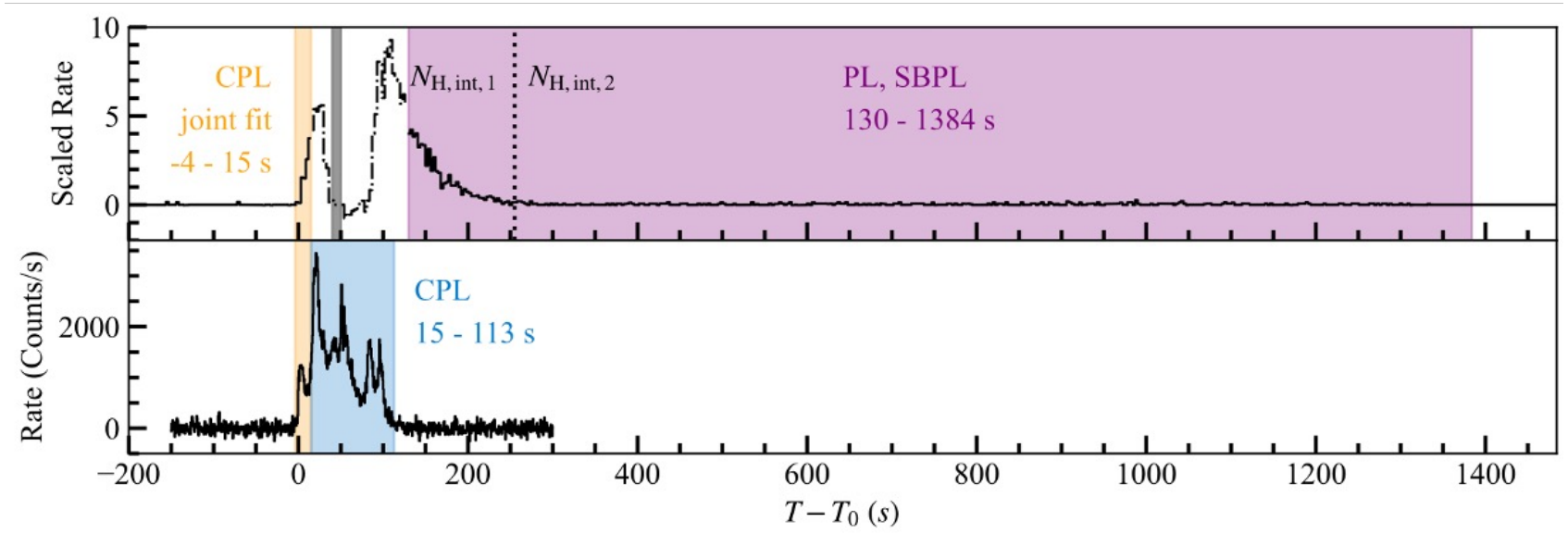

We fix $N_{H,int,1}$ at 3.73e22 cm^{-2} and $N_{H,int,2}$ at 6.39e21 cm^{-2} (best-fit from time-integrated spectrum) in light of:

1. time-dependent $N_{H,int}$ is expected because of photoionization and dust destruction*, and observed in the data
2. free $N_{H,int}$ in every time slice is not well constraint with large error bars
3. free or fixed intrinsic $N_{H,int}$ do not significantly affect spectral indices

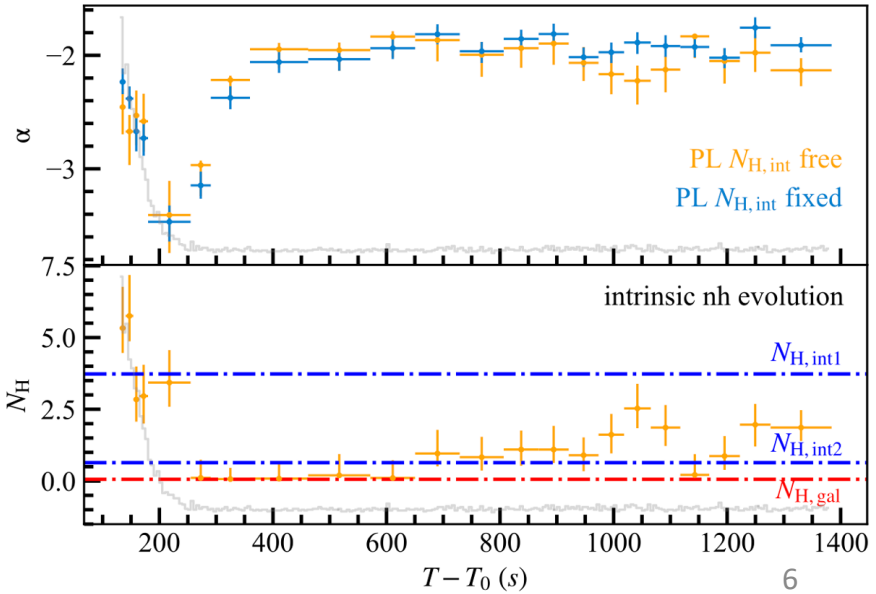

* ref: Lazzati et al., 2002, MNRAS; Perna et al., 2002, ApJ; Perna et al., 2003, ApJ; Lazzati et al., 2003, MNRAS; Campana et al. 2021, A&A;

EP250404a spectral fittings

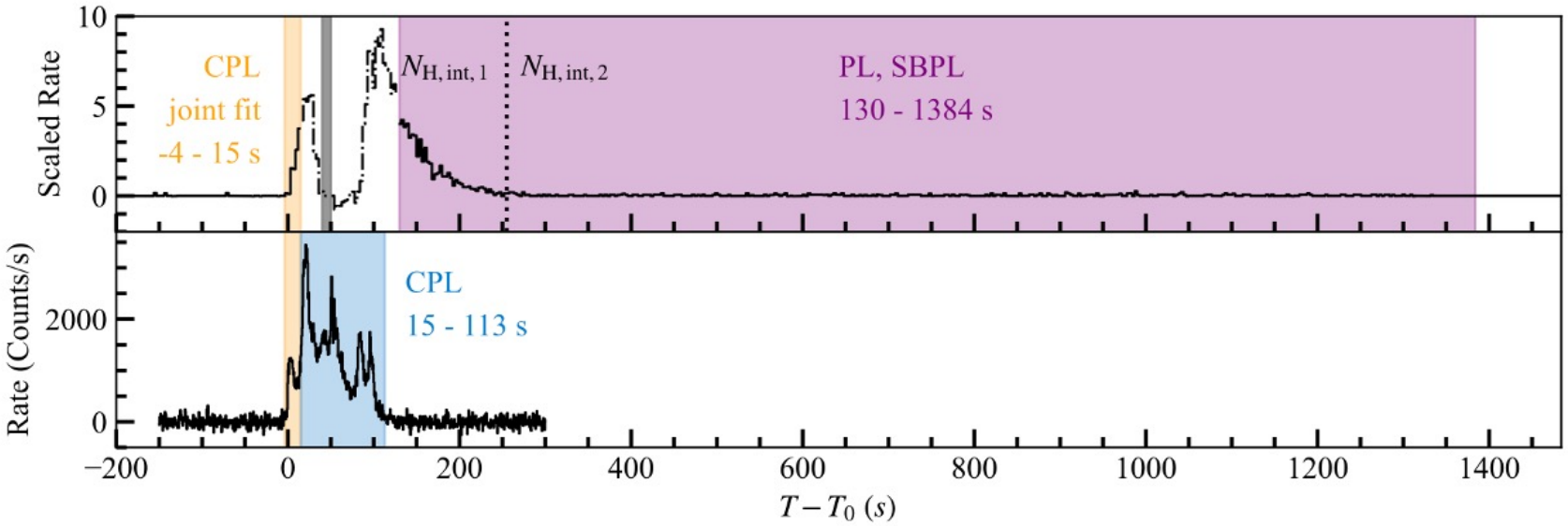

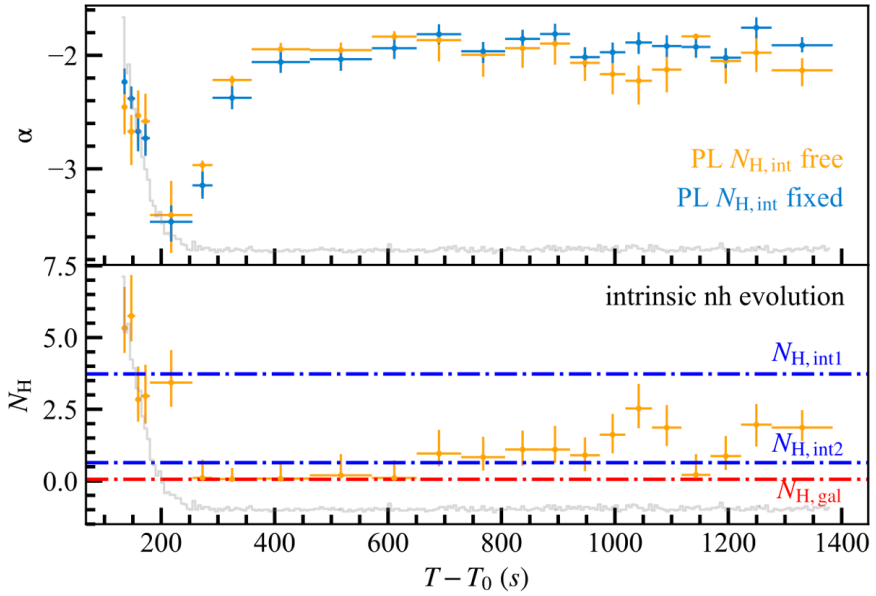

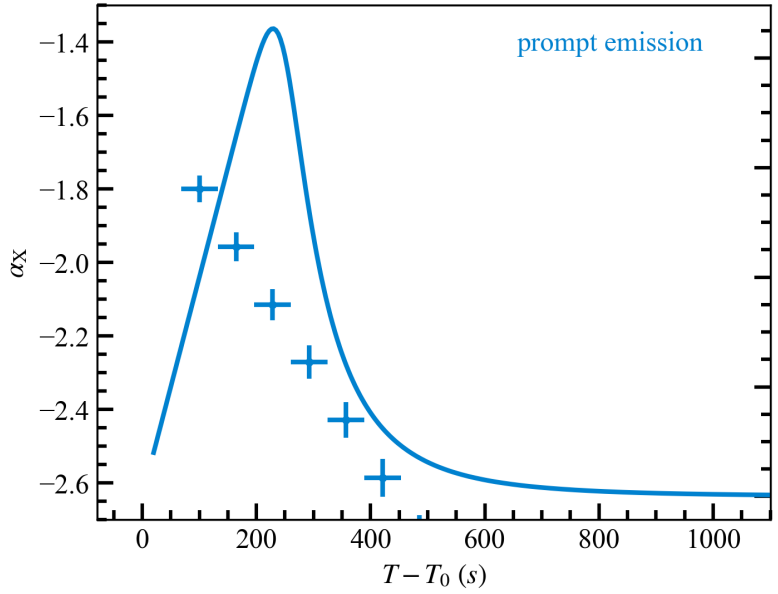

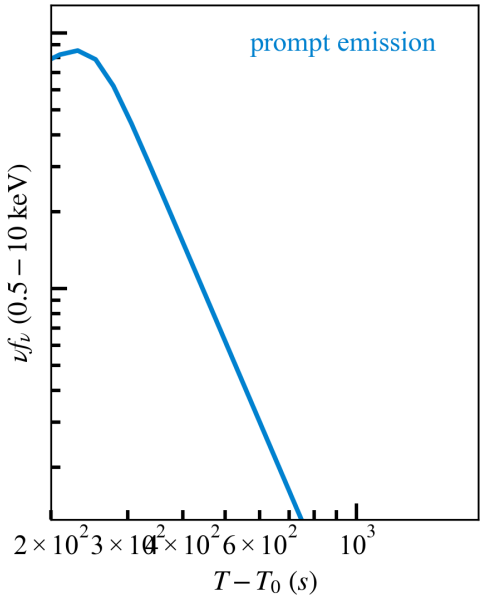

EP250404a spectral fittings

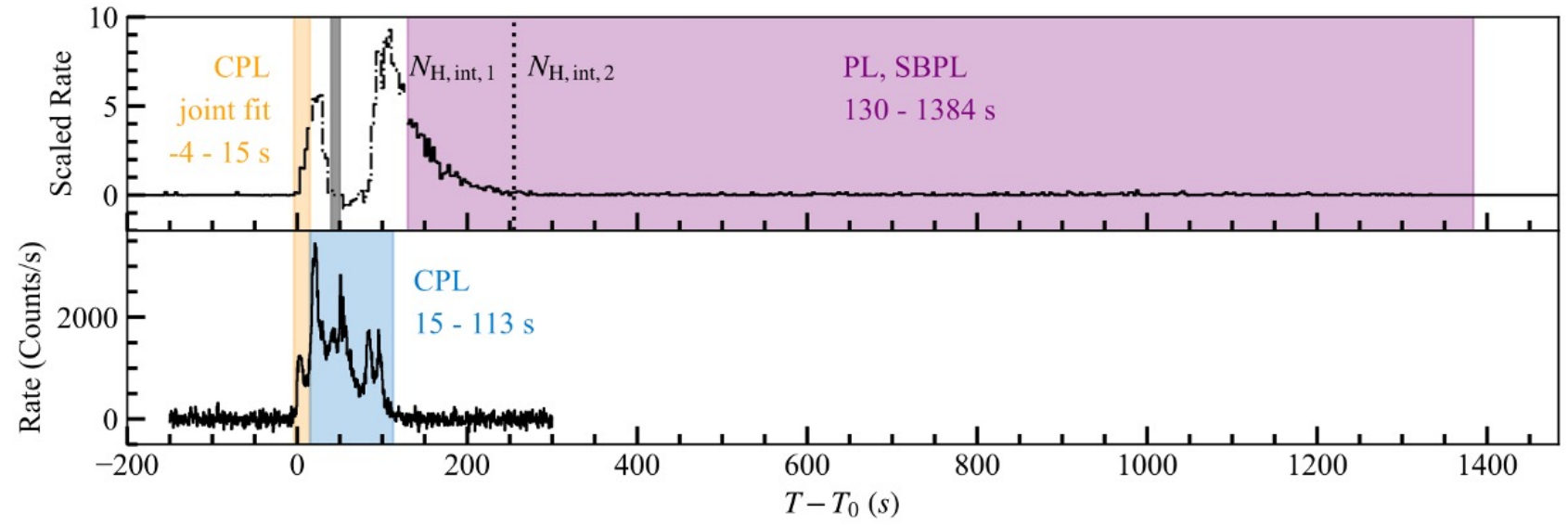

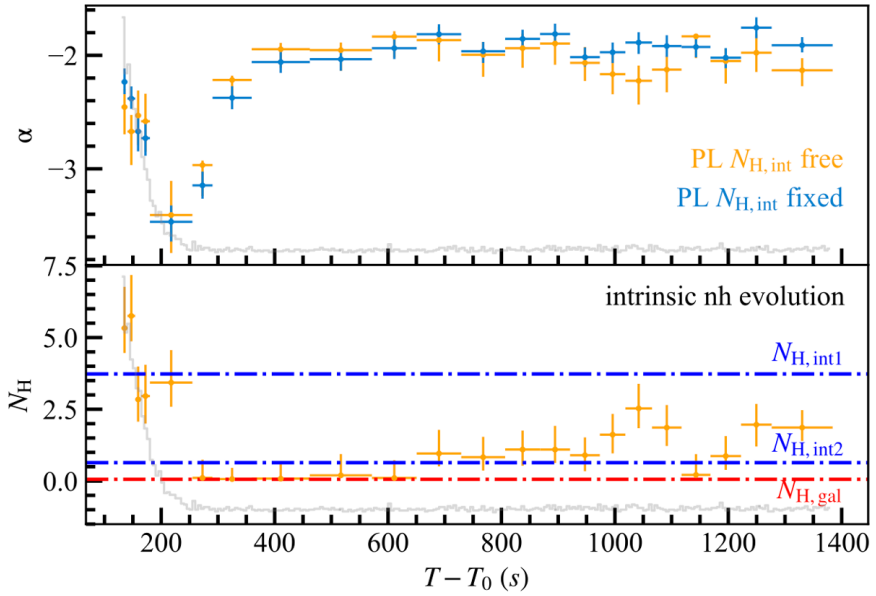

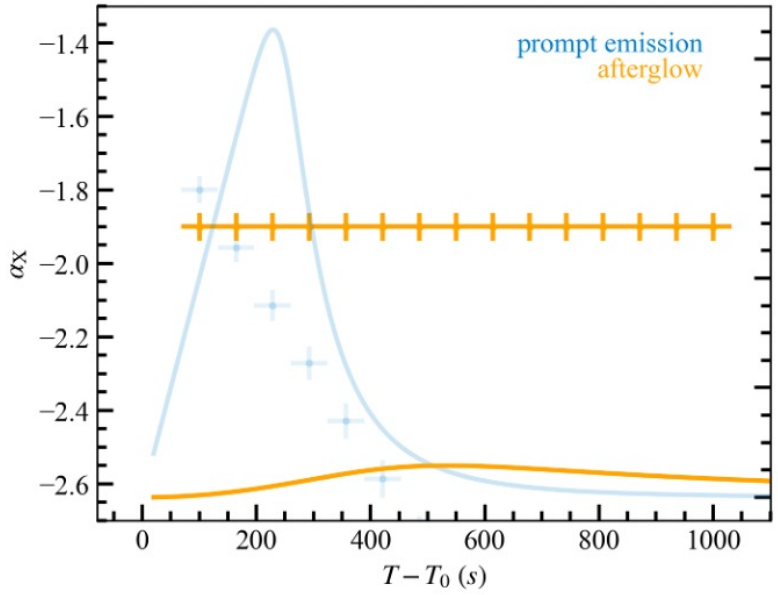

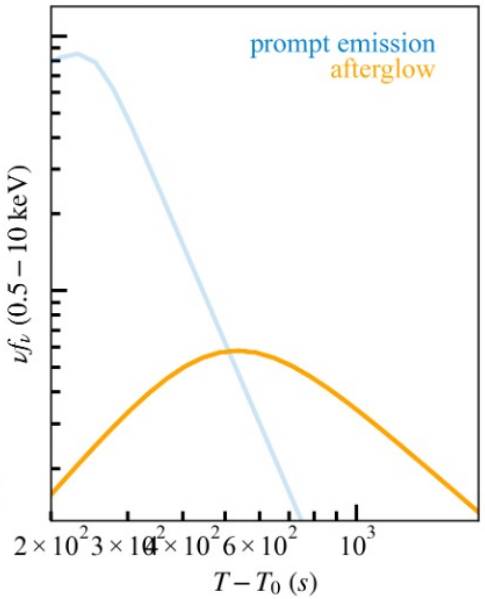

EP250404a spectral fittings

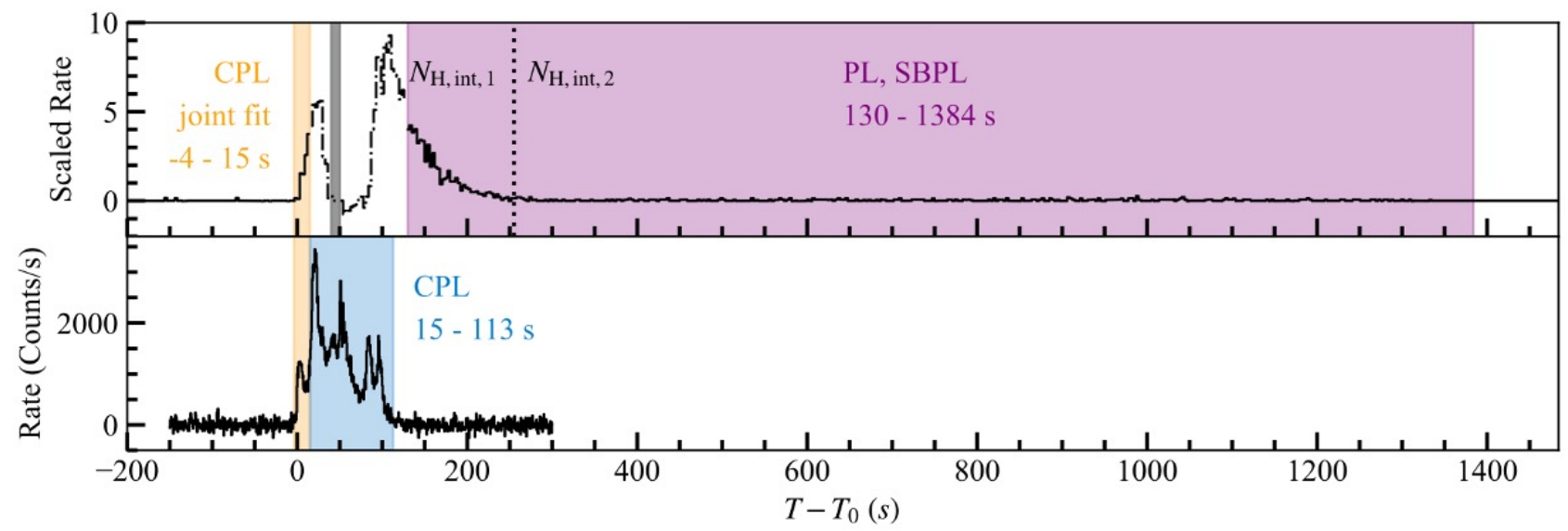

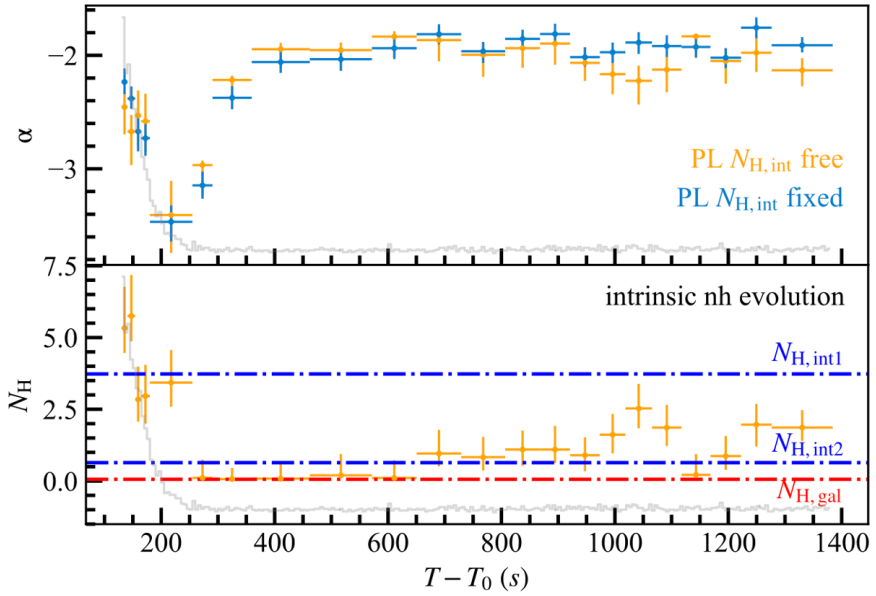

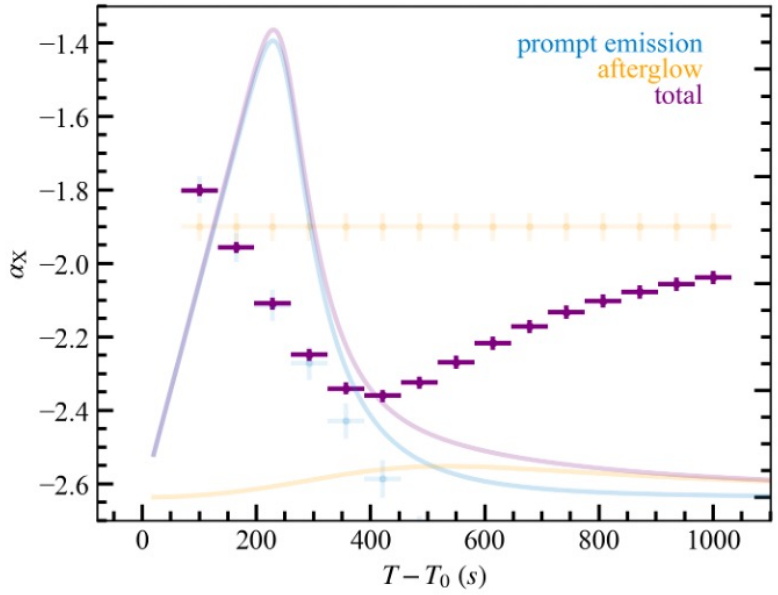

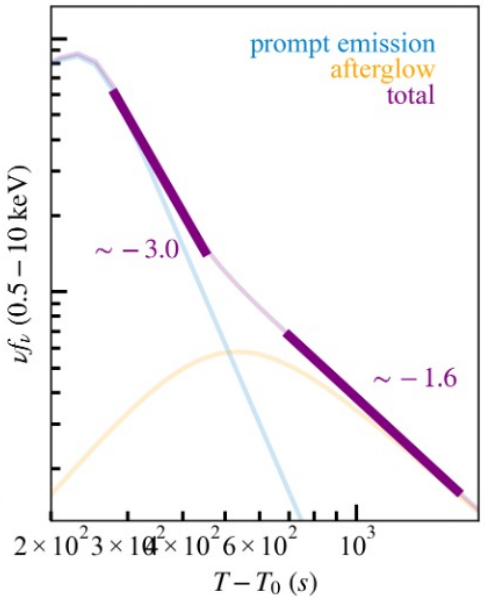

EP250404a spectral evolution

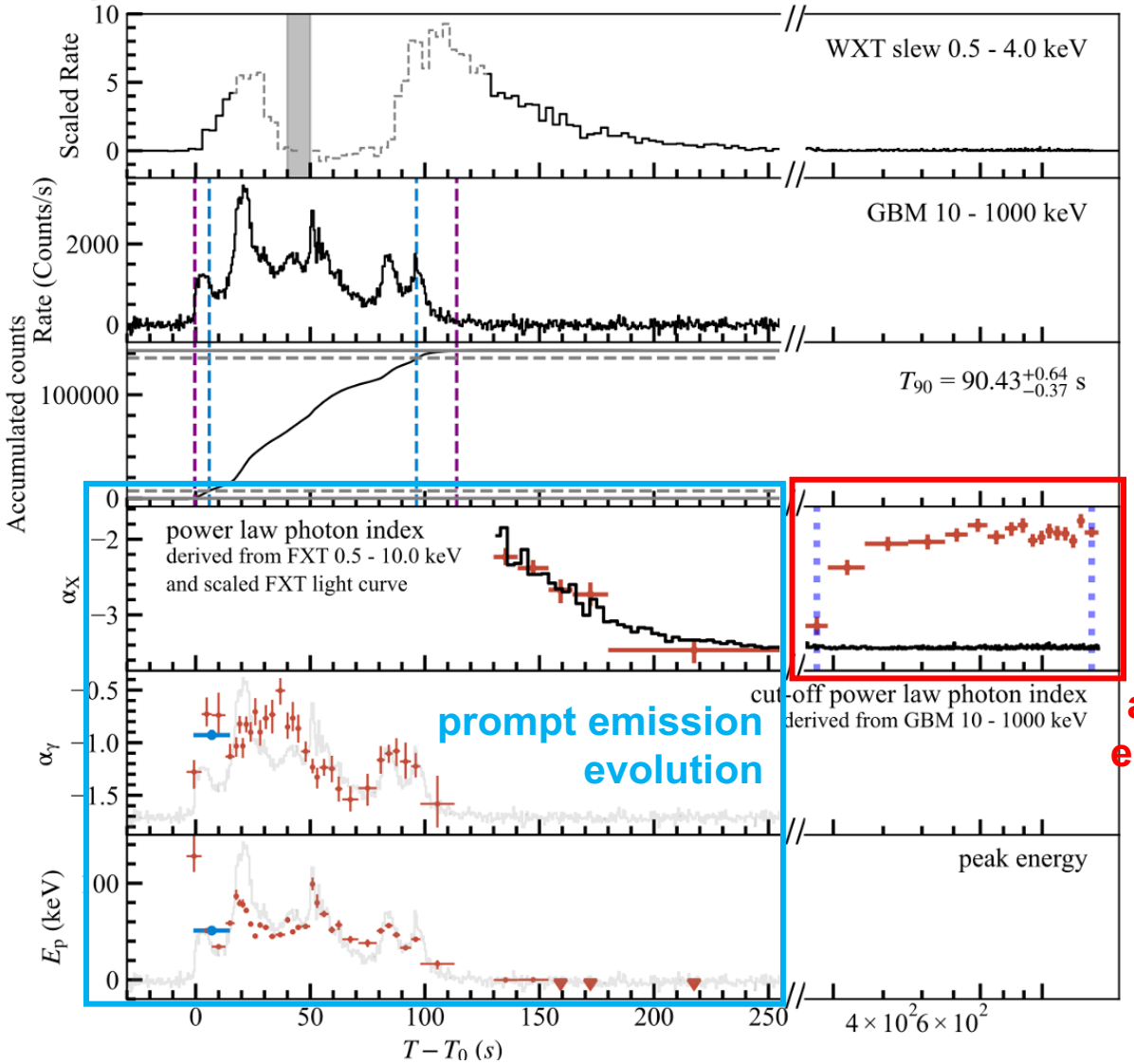

afterglow emergence

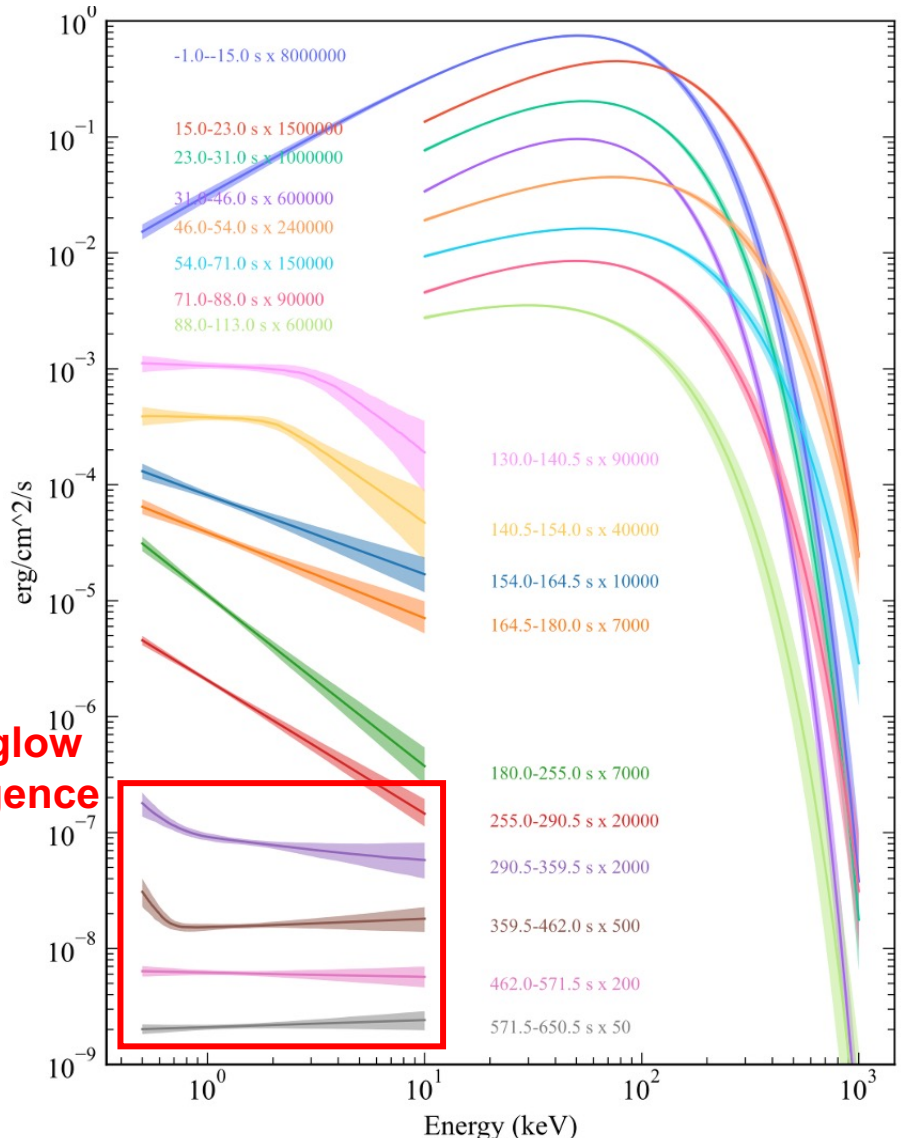

gamma-ray and X-ray light curves and spectral evolution

spectral energy distribution

EP250404a spectral evolution

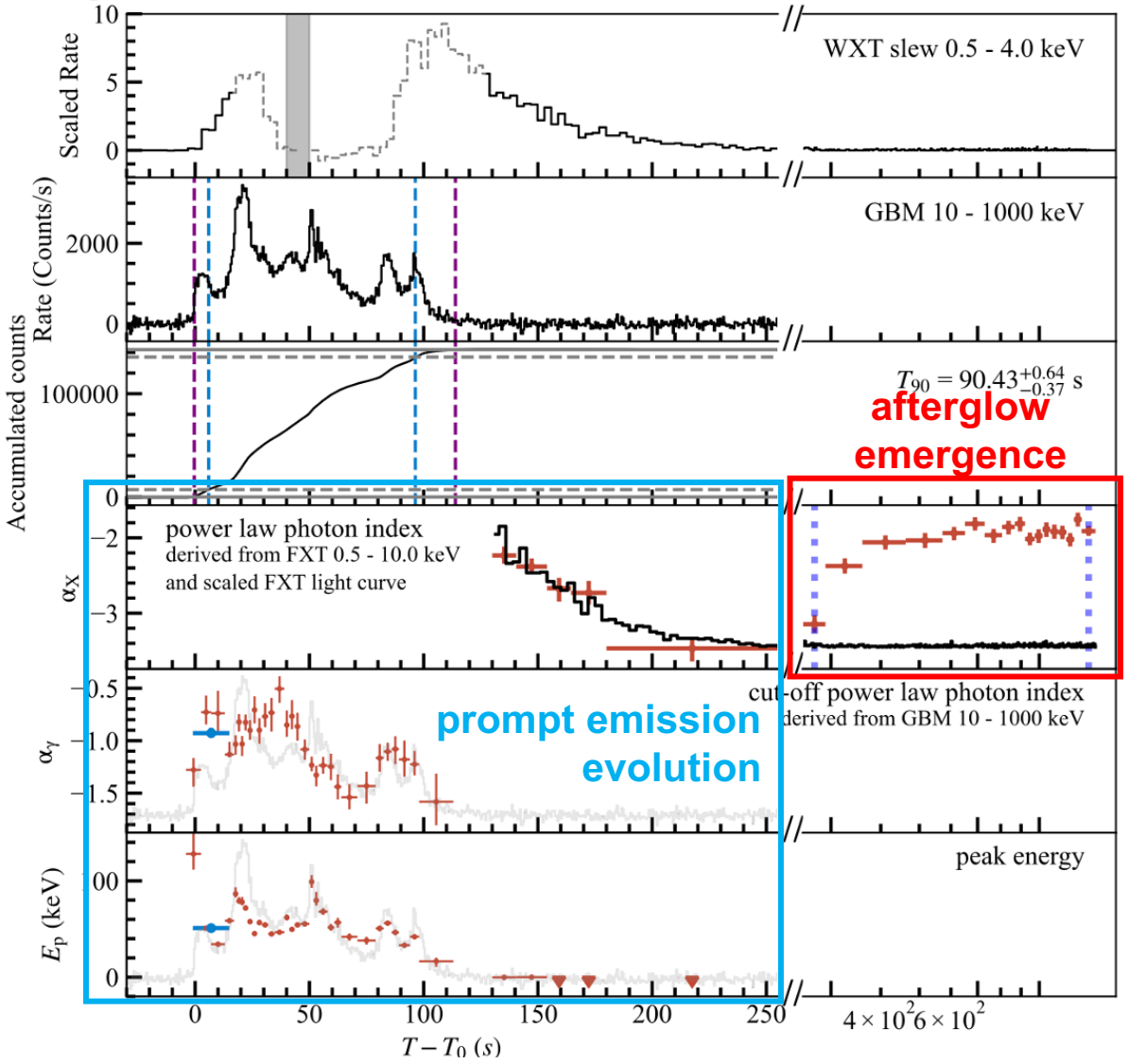

gamma-ray and X-ray light curves and spectral evolution

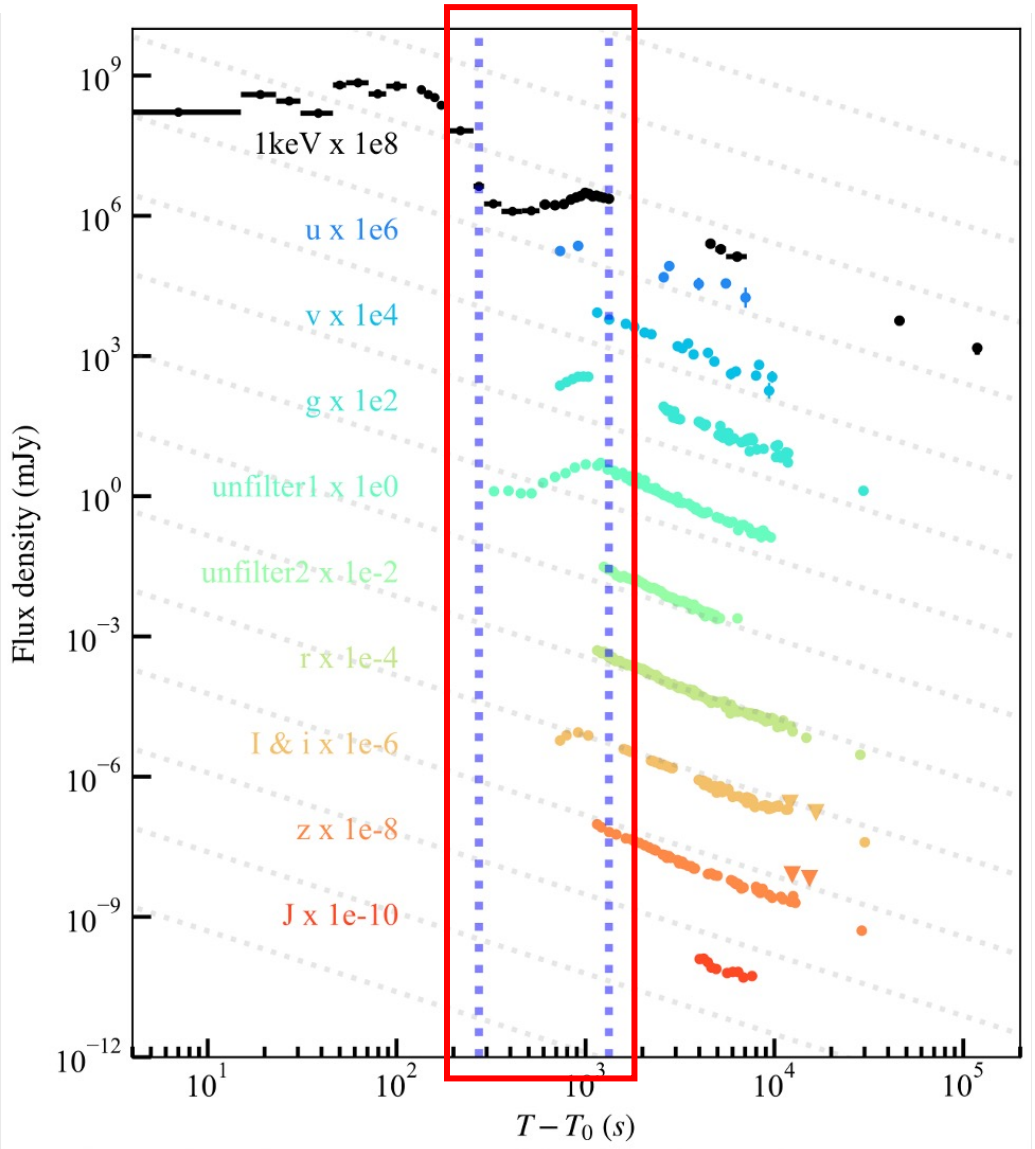

multiwavelength observations

EP250404a early multiwavelength observation

observations from

EP

Mephisto

SYSU

TNOT

BOOTES

Schmidt

NOT

HMT

ALT100C

ALT50D

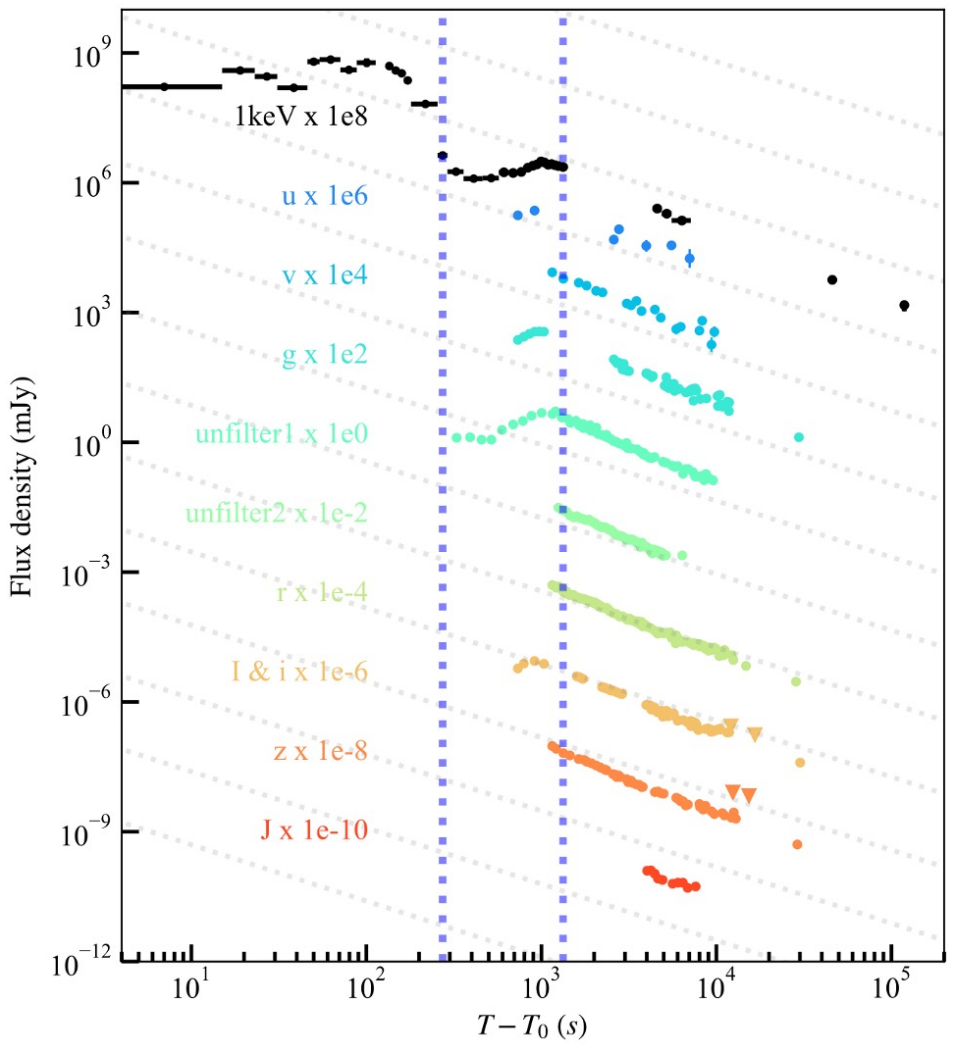

a sharp rise and a break in the decay,
likely contributions from reverse shock emission

EP250404a early multiwavelength observation

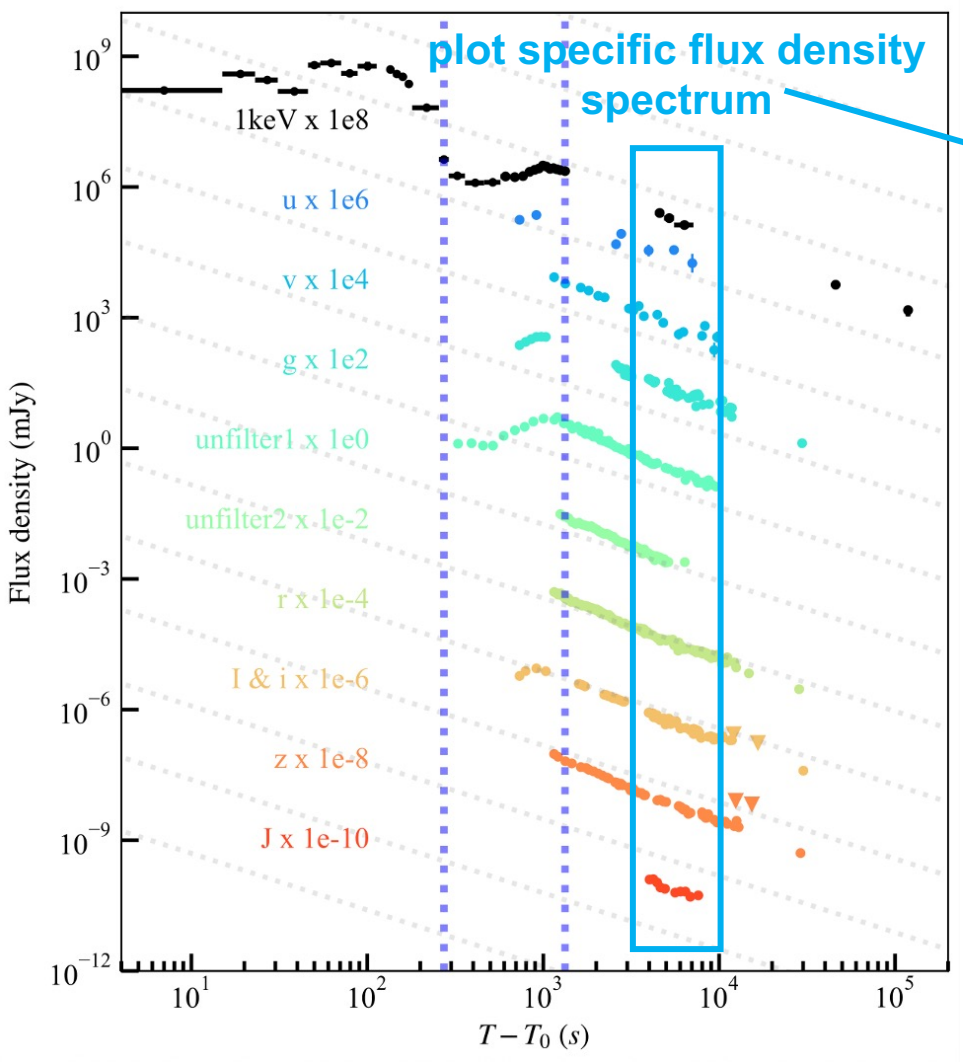

multiwavelength observations

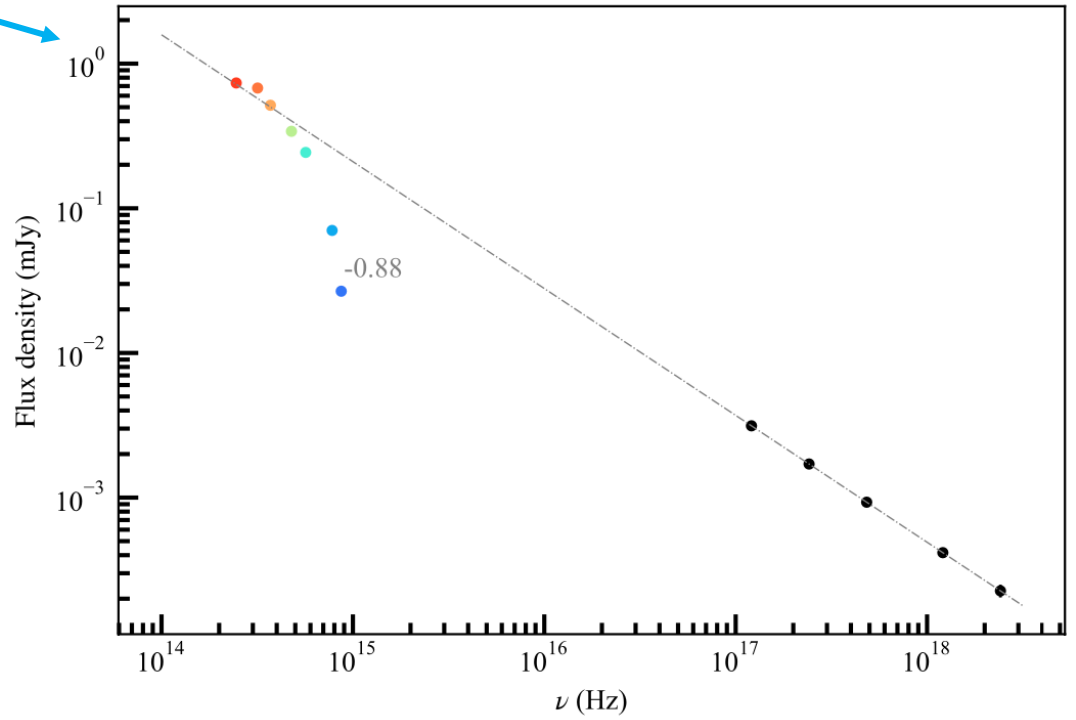

a clear drop in u, v and g band, likely host galaxy extinction

afterglow fit

afterglow models*

1. FS without u and v band
2. FS + RS without u and v band
3. FS with u, v, g band correction factors
4. FS + RS with u, v, g band correction factors

* ref: Zhang, B. 2018, The Physics of Gamma-Ray Bursts; Gao, H et al. 2013, NewAR; Lei, W.-H. et al. 2016, ApJ; Zhu, Z.-P. et al. 2023, ApJ;

afterglow fit without *u* and *v* band

Model	$\log E_{\rm k,iso}$ (erg)	$\log\Gamma_0$	$\theta_{\rm jet}$ (°)	$\log n_{18}$ ($\rm cm^{-3}$)	$p_{\rm f}$	$\log\epsilon_{\rm e,f}$	$\log\epsilon_{\rm B,f}$	$p_{\rm r}$
FS+RS	$53.07^{+0.21}_{-0.01}$	$1.75^{+0.07}_{-0.04}$	$6.96^{+1.06}_{-0.56}$	$2.43^{+0.52}_{-0.14}$	$2.68^{+0.03}_{-0.01}$	$-0.52^{+0.00}_{-0.07}$	$-5.15^{+0.05}_{-0.44}$	$2.26^{+0.04}_{-0.09}$
FS	$53.71^{+0.54}_{-0.21}$	$2.91^{+0.03}_{-0.31}$	$9.81^{+0.09}_{-0.74}$	$3.81^{+0.25}_{-0.87}$	$2.82^{+0.04}_{-0.01}$	$-0.51^{+0.05}_{-0.58}$	$-6.81^{+0.84}_{-0.04}$	-
Model	$\log\epsilon_{\rm e,r}$	$\log\epsilon_{\rm B,r}$	logv	$\log f_u$	$\log f_v$	$\log f_g$	χ^2/dof	BIC
FS+RS	$-0.66^{+0.08}_{-0.11}$	$-4.01^{+0.03}_{-0.44}$	$-0.57^{+0.02}_{-0.00}$	-	-	-	322.69/314	160.20
FS	-	-	$-0.51^{+0.03}_{-0.01}$	-	-	-	330.84/317	228.74

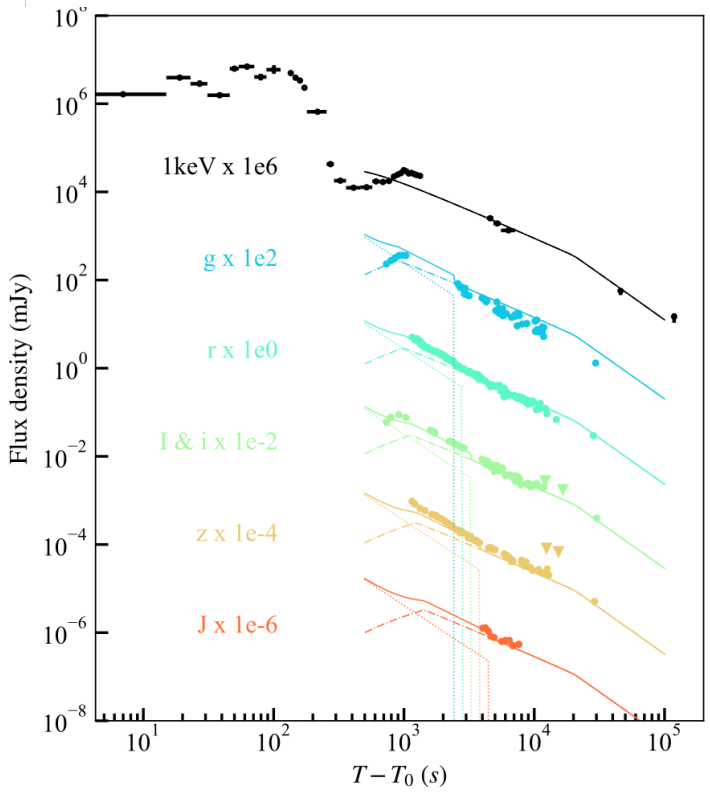

forward shock + reverse shock

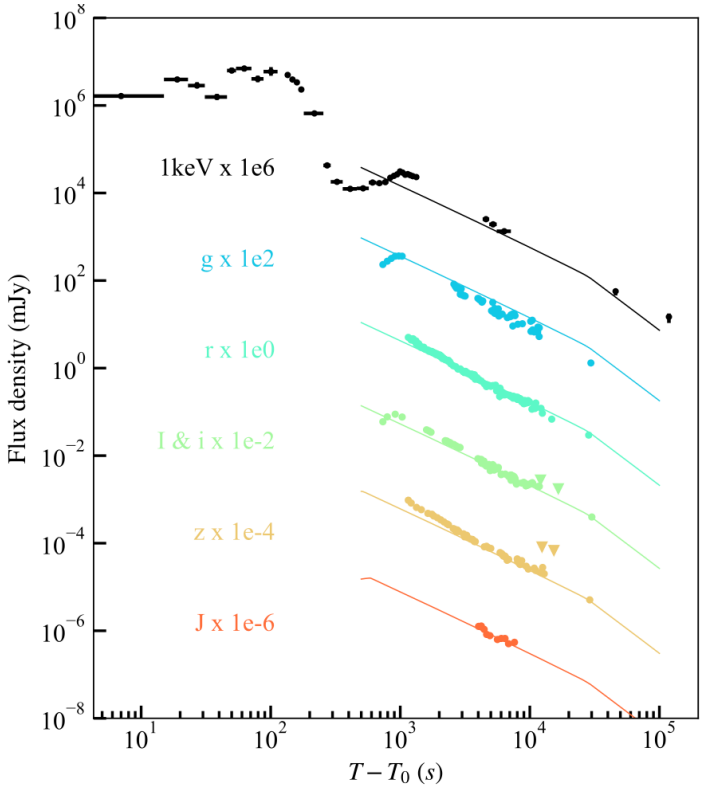

forward shock

afterglow fit with *u*, *v* and *g* band correction factors

Model	$\log E_{\rm k,iso}$ (erg)	$\log\Gamma_0$	$\theta_{\rm jet}$ (°)	$\log n_{18}$ ($\rm cm^{-3}$)	$p_{\rm f}$	$\log\epsilon_{\rm e,f}$	$\log\epsilon_{\rm B,f}$	$p_{\rm r}$
FS+RS*	$55.52^{+0.23}_{-0.78}$	$2.38^{+0.06}_{-0.23}$	$6.04^{+2.74}_{-2.11}$	$-1.08^{+1.30}_{-0.46}$	$2.86^{+0.01}_{-0.04}$	$-2.10^{+0.66}_{-0.04}$	$-4.11^{+0.39}_{-1.25}$	$2.64^{+0.05}_{-0.01}$
FS*	$53.35^{+0.54}_{-0.02}$	$2.89^{+0.06}_{-0.24}$	$9.67^{+0.27}_{-0.23}$	$3.52^{+0.65}_{-0.15}$	$2.81^{+0.02}_{-0.01}$	$-0.28^{+0.00}_{-0.55}$	$-6.32^{+0.24}_{-0.54}$	-
Model	$\log\epsilon_{\rm e,r}$	$\log\epsilon_{\rm B,r}$	logv	$\log f_u$	$\log f_v$	$\log f_g$	χ^2/dof	BIC
FS+RS*	$-0.60^{+0.34}_{-0.38}$	$-5.45^{+0.73}_{-0.32}$	$-0.84^{+0.02}_{-0.02}$	$-1.14^{+0.06}_{-0.01}$	$-0.57^{+0.02}_{-0.02}$	$-0.20^{+0.00}_{-0.02}$	353.41/336	-178.19
FS*	-	-	$-0.64^{+0.02}_{-0.01}$	$-1.13^{+0.07}_{-0.02}$	$-0.55^{+0.03}_{-0.03}$	$-0.22^{+0.01}_{-0.02}$	345.55/339	77.11

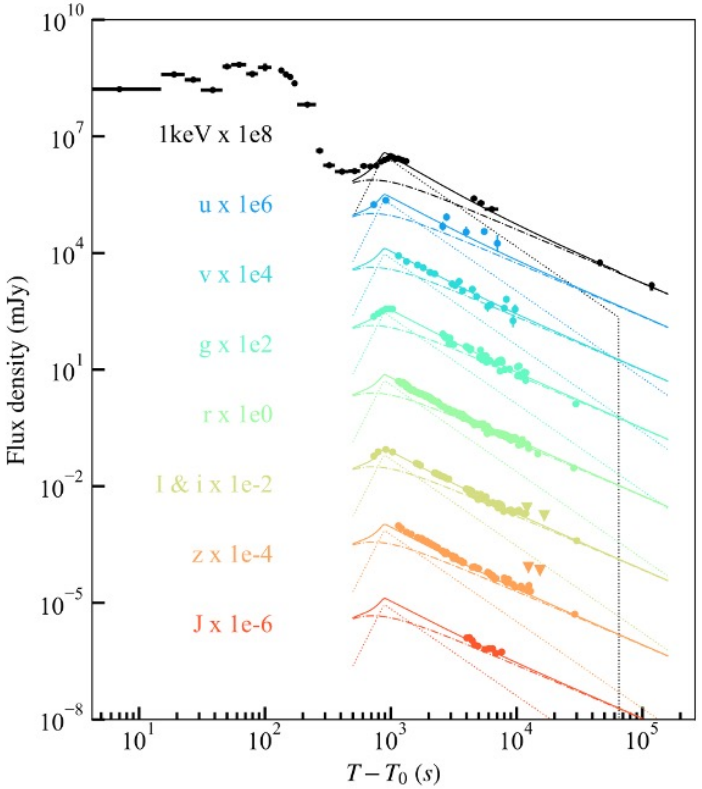

forward shock + reverse shock (best)

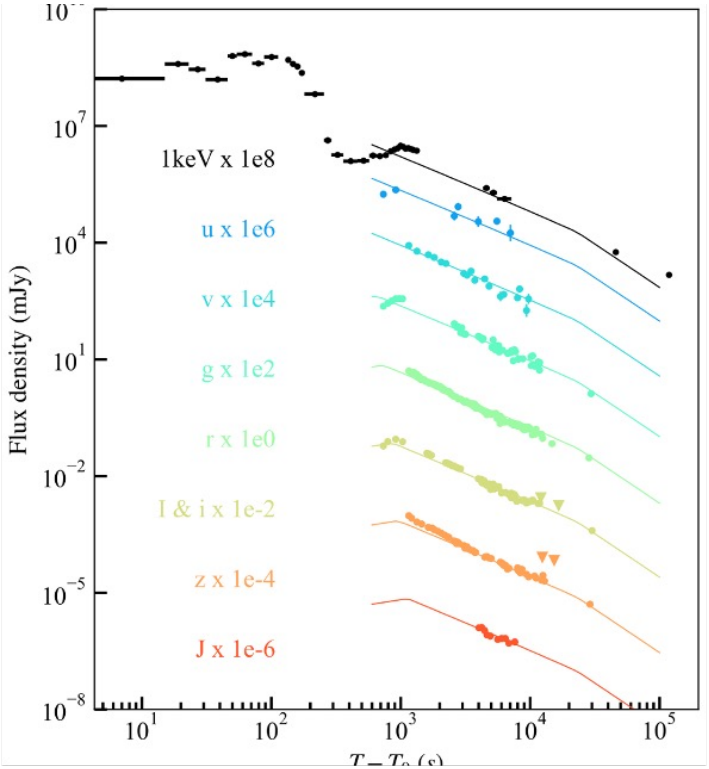

forward shock

Final afterglow fit: FS + RS with *u*, *v*, *g* band correction factors

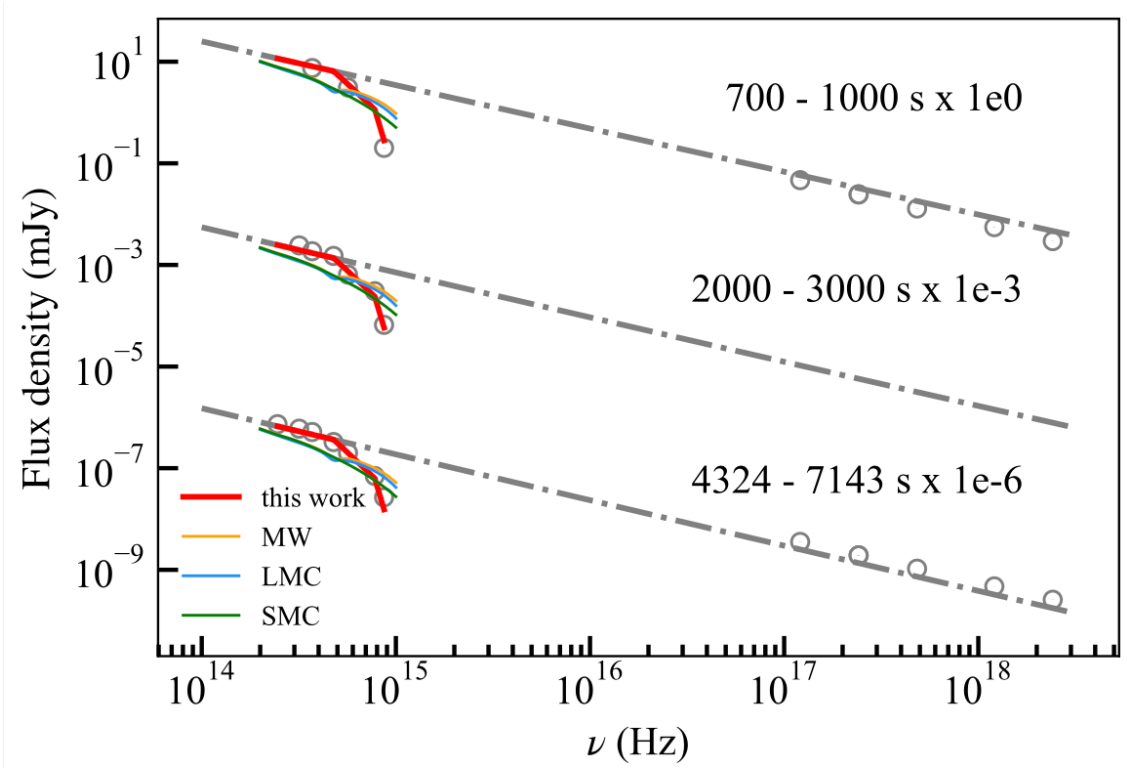

partial extinction curve

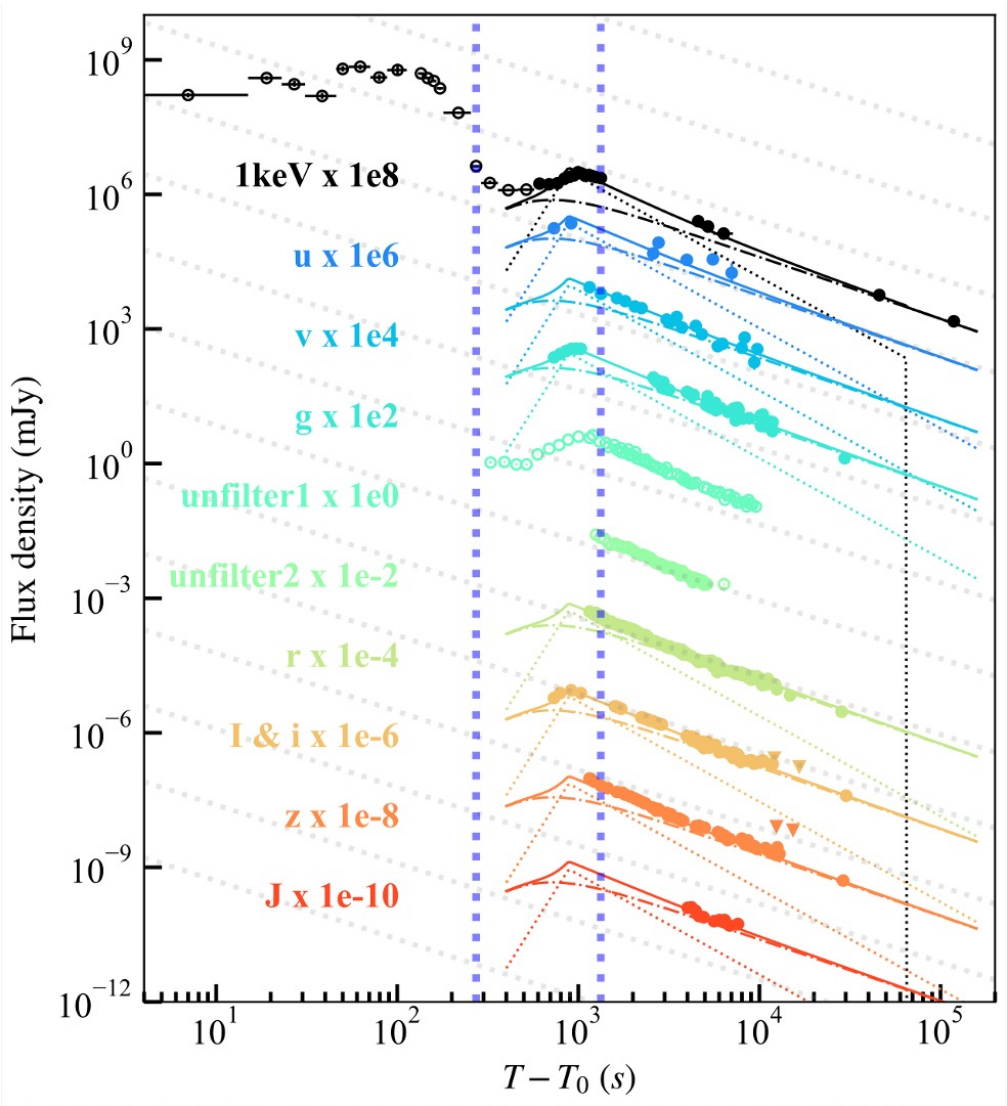

FS+RS model with extinction corrections

We indeed found the afterglow emergence

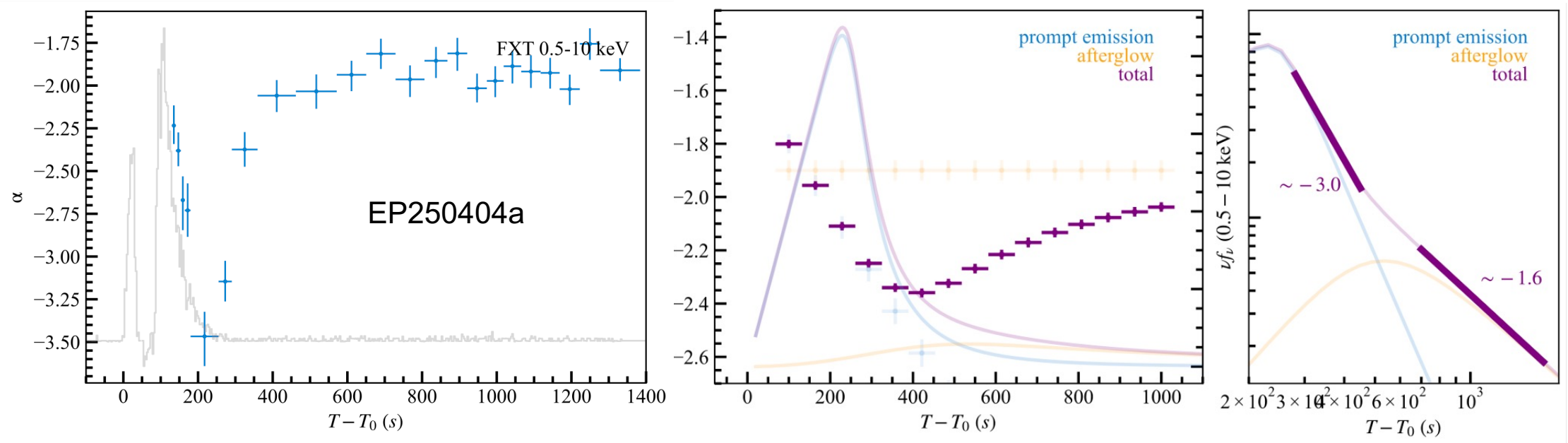

This case: afterglow emerges in the long-duration emission tail

- a characteristic soft–hard–flat pattern of α
- flux showing two distinct phases: steep decay + normal decay, e.g., EP250404a

Other cases?

Even more interesting/useful

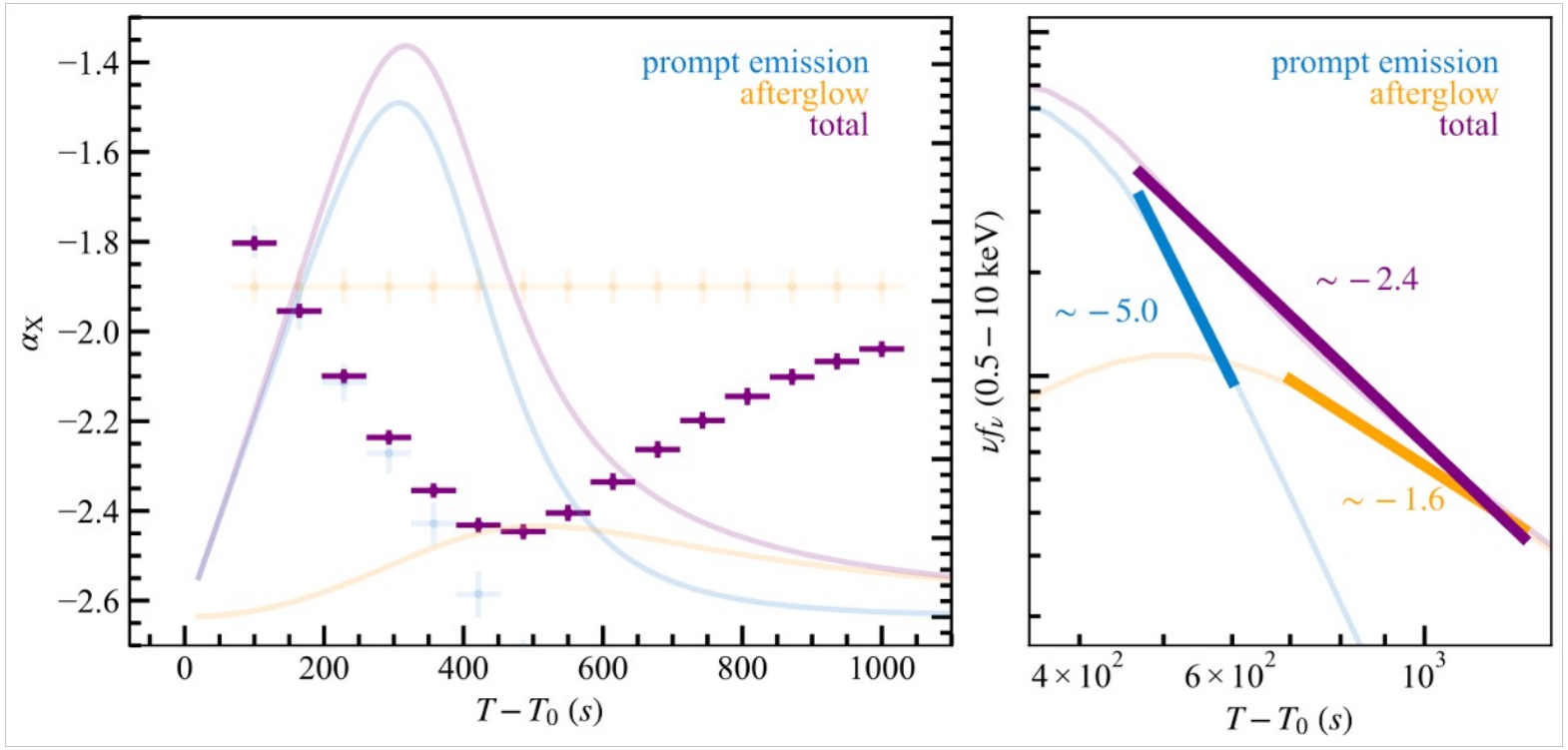

The prompt and afterglow emissions are superimposed and of comparable intensity, $\alpha_{prompt} < \alpha_{afterglow}$

- a characteristic soft–hard–flat pattern of α
- one may be able to separate the components, e.g., EP250304a

Even more interesting/useful

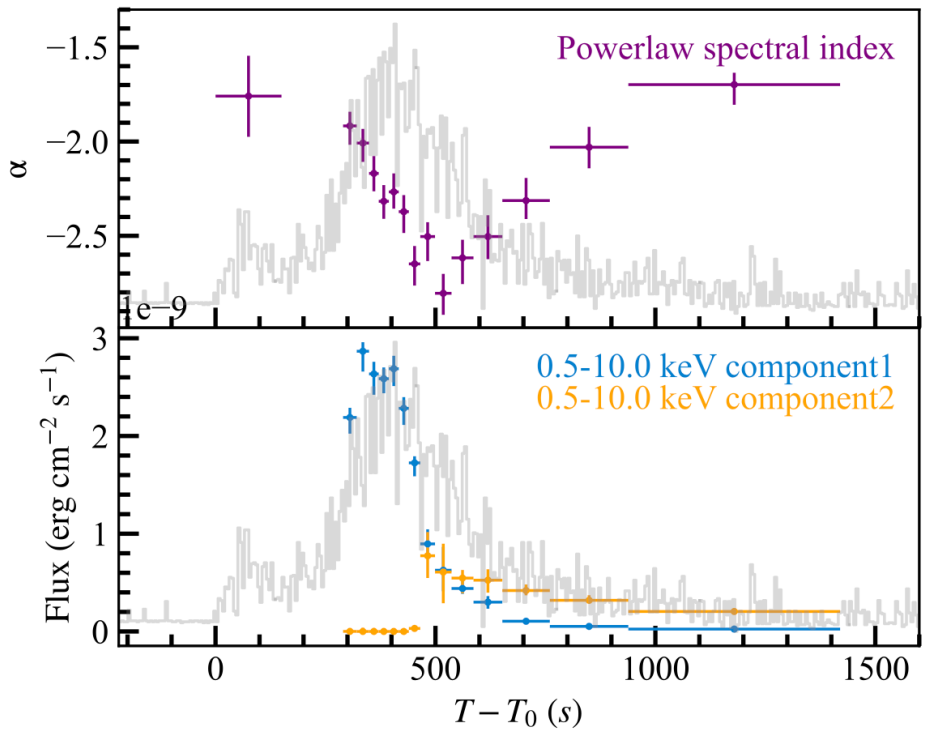

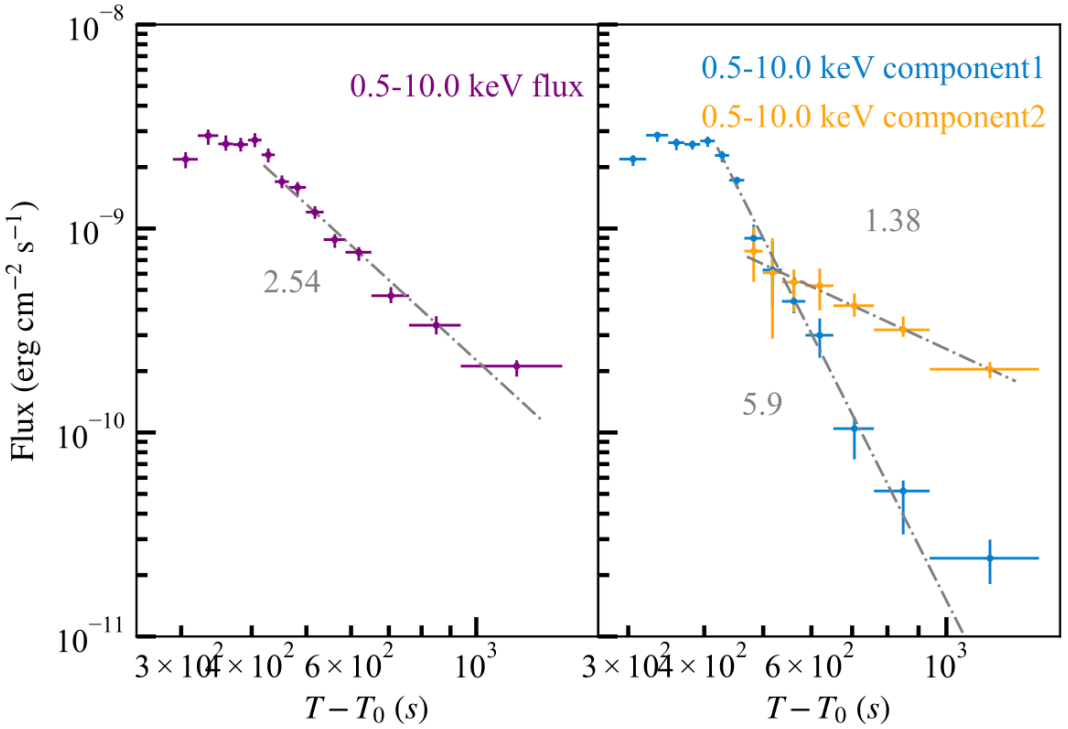

The prompt and afterglow emissions are superimposed and of comparable intensity, $\alpha_{prompt} < \alpha_{afterglow}$

- a characteristic soft–hard–flat pattern of α
- one may be able to separate the components, e.g., EP250304a

Indistinguishable

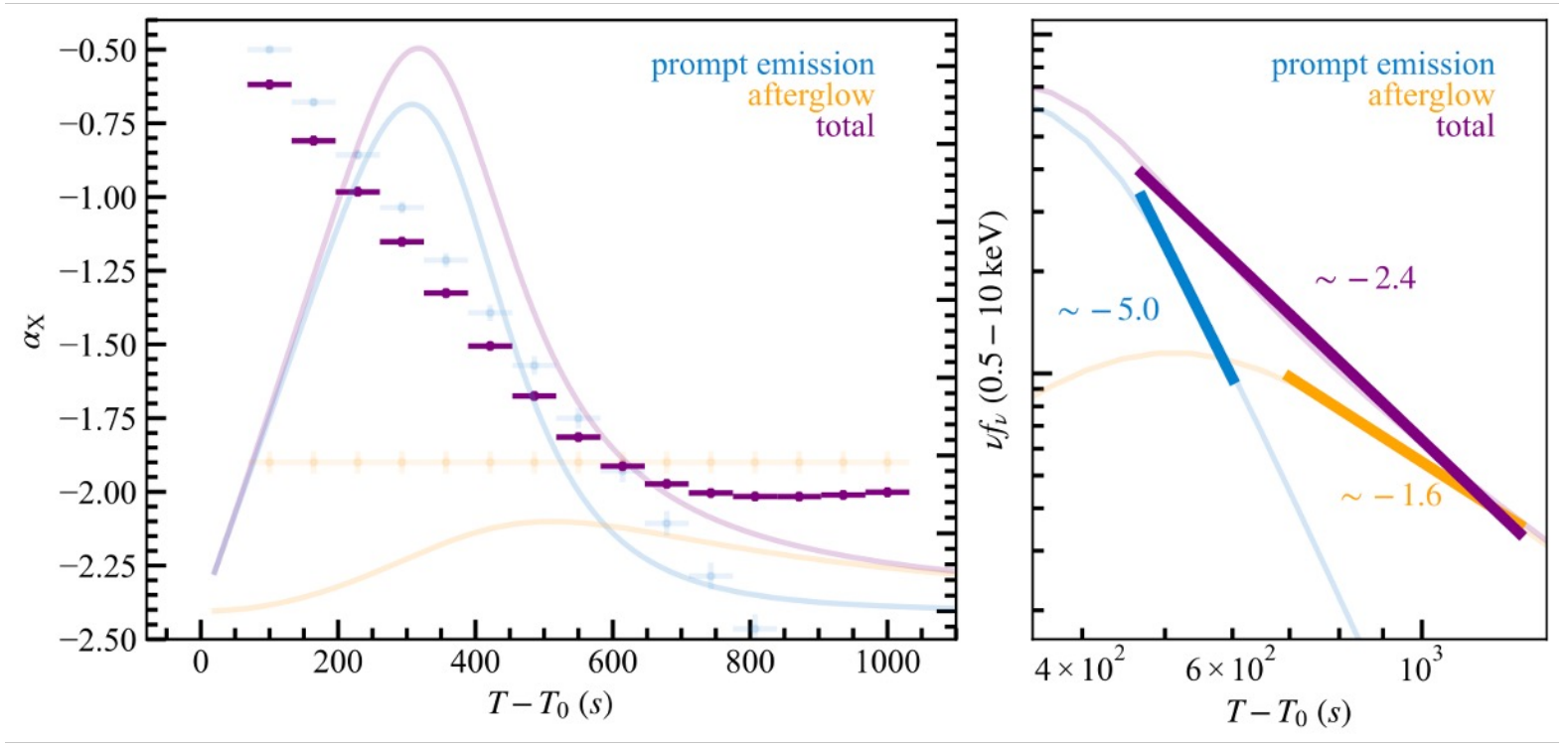

α_{prompt} > $\alpha_{afterglow}$ when the afterglow begins to dominate

- a gradual softening of α
- hard to tell the components of the spectra

Transition Cases

practical criterion for identifying GRBs in fast X-ray transients, even when the gamma-ray counterpart and the flux breaks are absent

Case I

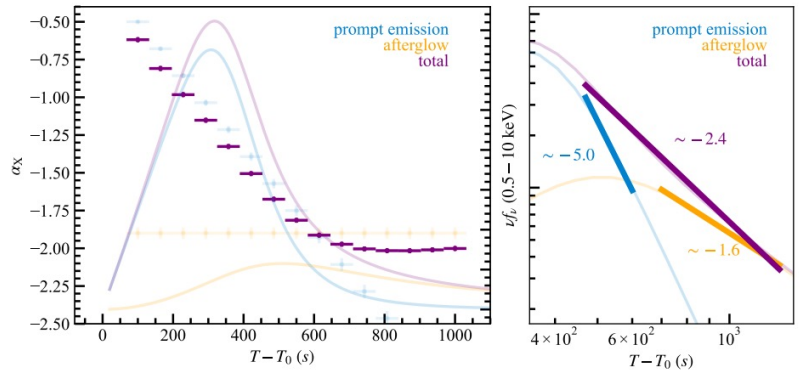

Case II

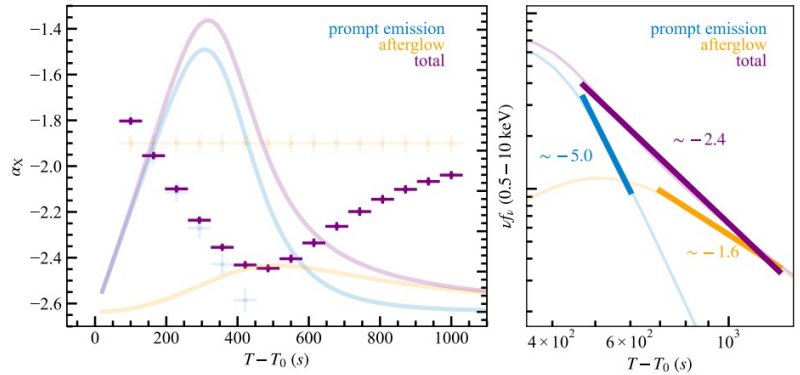

Case III

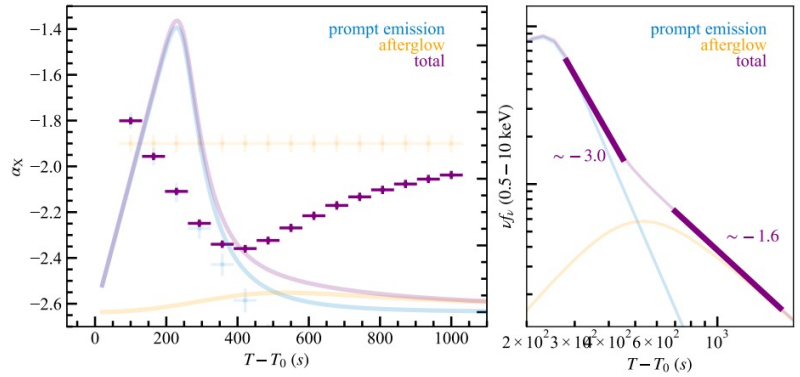

Summary

- EP250404a was triggered by **EP/WXT** and has a long-duration tail lasting over 1000 s observed by **EP/FXT**. **Fermi/GBM** observed a gamma-ray counterpart with T_{90} ~ 90.43 s.
- Significant **spectral evolution** is observed in the prompt emission of GRB 250404A/EP250404a, with the peak energy decaying from gamma-ray band to X-ray band. The spectral indices evolve from hard to soft.
- From the X-ray continuous emission, we have observed **a spectral hardening starting from ~ 255 s**, which marks the afterglow emergence following the steep decay phase of the prompt emission.
- We have fitted the rich early-time multiwavelength follow-up observations with **forward and reverse shock model** with host extinction correction factors. We therefore derived the partial host extinction curve of this source.
- **We propose that the significant spectral hardening observed in the fast X-ray transients serves as an indicator for the afterglow emergence.** We discuss three scenarios of the transition from the prompt emission to afterglow in the long-duration fast X-ray transients.

Summary of the observed properties of GRB250404A/EP250404a

Observed Properties	EP250404a
Redshift	1.88
Galactic $N_{\rm H}$ ($\rm cm^{-2}$)	6.00×10^{20}
Intrinsic $N_{\rm H}$ ($\rm cm^{-2}$)	$3.73^{+0.35}_{-0.45} \times 10^{22}$ $6.39^{+1.61}_{-1.31} \times 10^{21}$
Gamma-rays (10–1000 keV)	
T_{90} (s)	$90.43^{+0.64}_{-0.37}$
Spectral index α_γ	$-1.15^{+0.02}_{-0.02}$
Peak energy (keV)	$55.34^{+0.64}_{-0.51}$
Peak flux ($\rm erg\,cm^{-2}\,s^{-1}$)	$8.62^{+0.33}_{-0.28} \times 10^{-7}$
Total fluence ($\rm erg\,cm^{-2}$)	$3.37^{+0.01}_{-0.01} \times 10^{-5}$
Peak luminosity ($\rm erg\,s^{-1}$)	$7.81^{+0.30}_{-0.25} \times 10^{51}$
Isotropic energy (erg)	$3.05^{+0.01}_{-0.01} \times 10^{53}$
X-rays (0.5–10.0 keV)	
Duration (s)	~ 300
Spectral index* $\alpha_{\rm X}$	$-2.59^{+0.05}_{-0.06}$
Flux* ($\rm erg\,cm^{-2}\,s^{-1}$)	$9.61^{+0.26}_{-0.23} \times 10^{-9}$
Total fluence* ($\rm erg\,cm^{-2}$)	$1.20^{+0.01}_{-0.01} \times 10^{-6}$
Isotropic energy* (erg)	$1.09^{+0.01}_{-0.01} \times 10^{52}$

* The parameters are derived in the time range 130–255 s.

Cases with observation support

EP samples showing spectral hardening

EP250223a

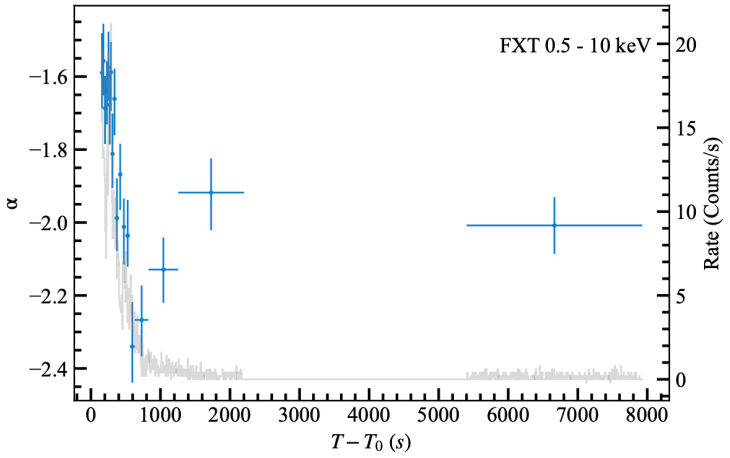

EP250304a

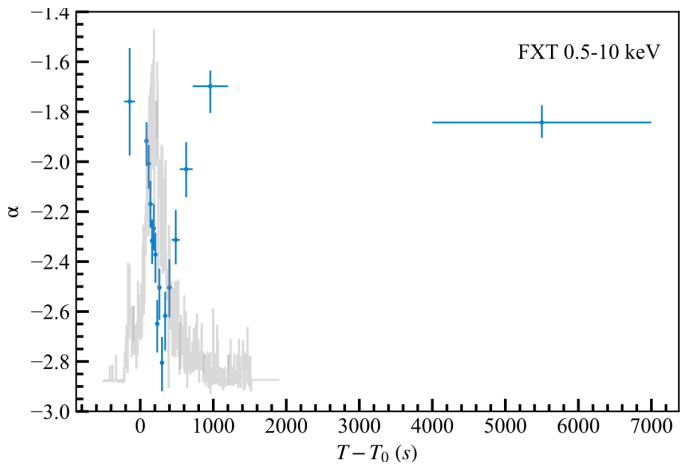

EP250404a

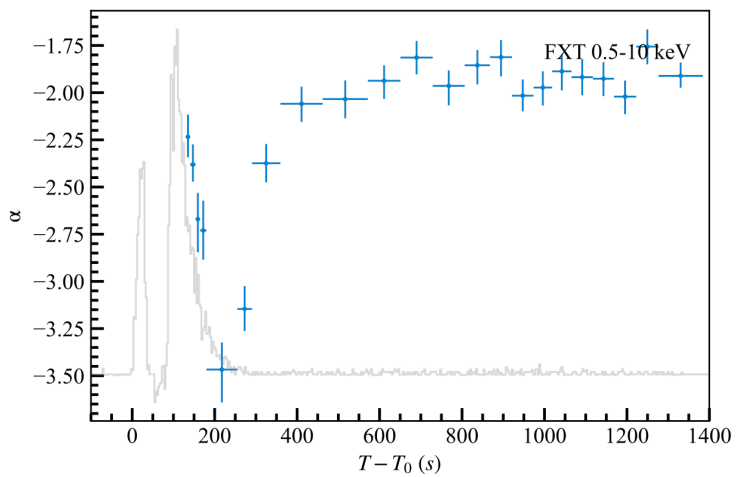

Pile-up reduction

EP250404a pile-up reduction

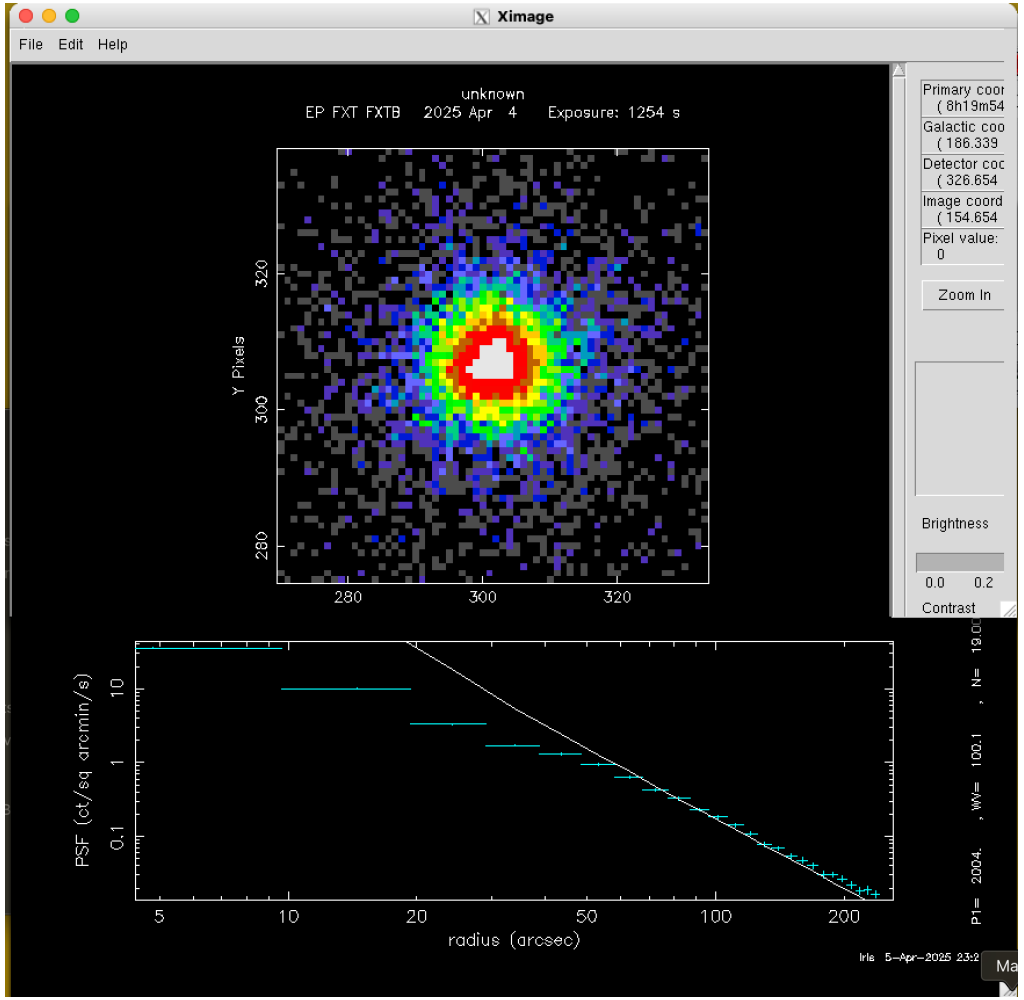

pile-up in FXT-A within 70 arcsec of the source from T_0 + 130 – 255 s

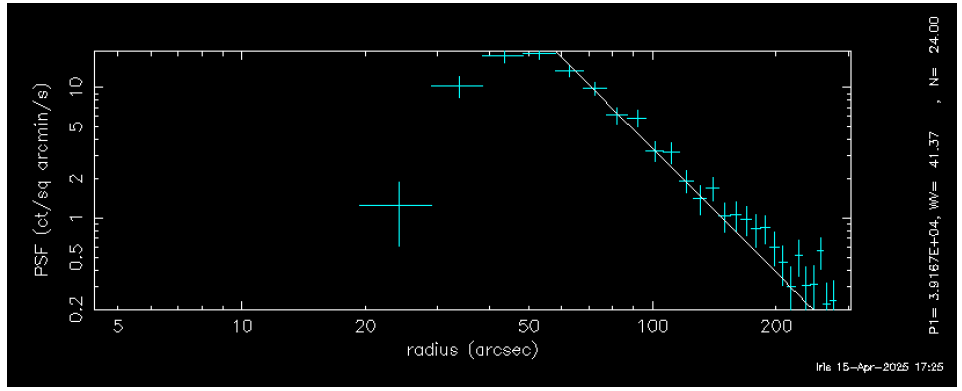

FXT-B full frame mode suffered from pile-up for ~ 7000 s

Data selection and reduction:

Time range	Source region	detector
130 – 255 s	70” – 150” annulus	FXT-A
255 – 7143 s	40” circle	FXT-A
44412 – 122326 s	40” circle	FXT-A and -B

Spectral fitting models

EP250404a model comparison

low energy break?

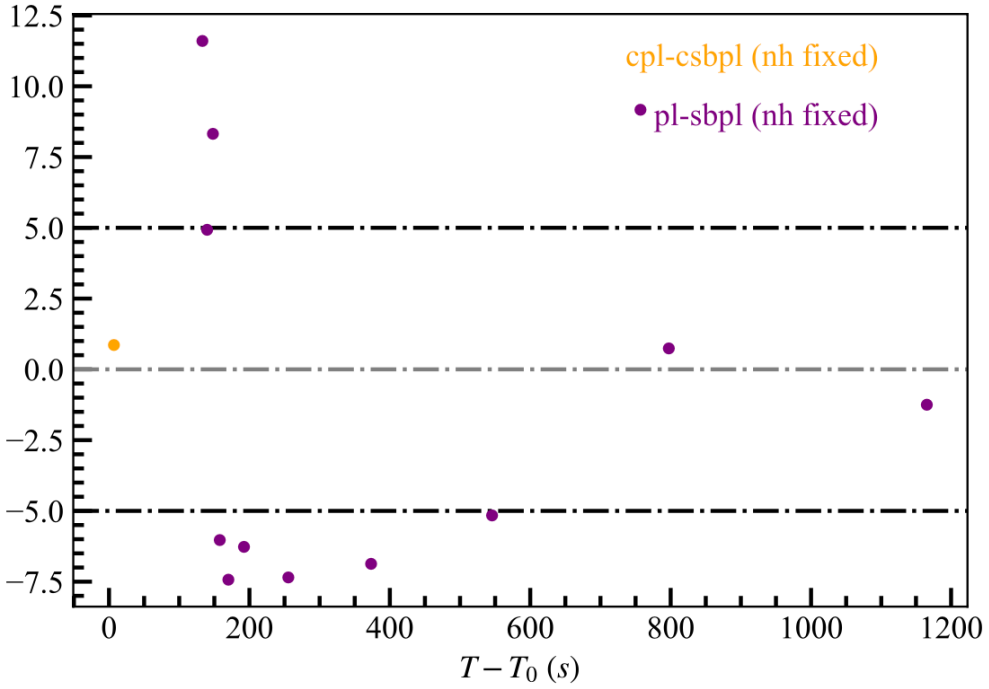

a low energy break is preferred between ~100-150 s

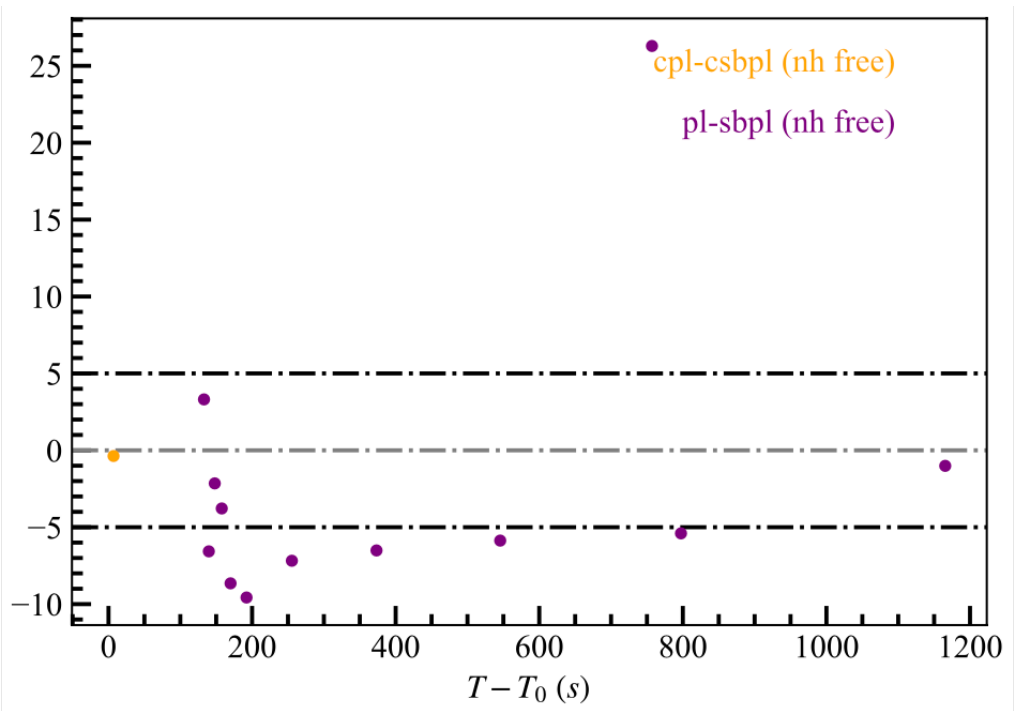

a low energy break is not preferred after ~150 s

There is likely an Epeak evolution.

EP250404a model comparison

fix or free nh? (statistically indistinguishable)

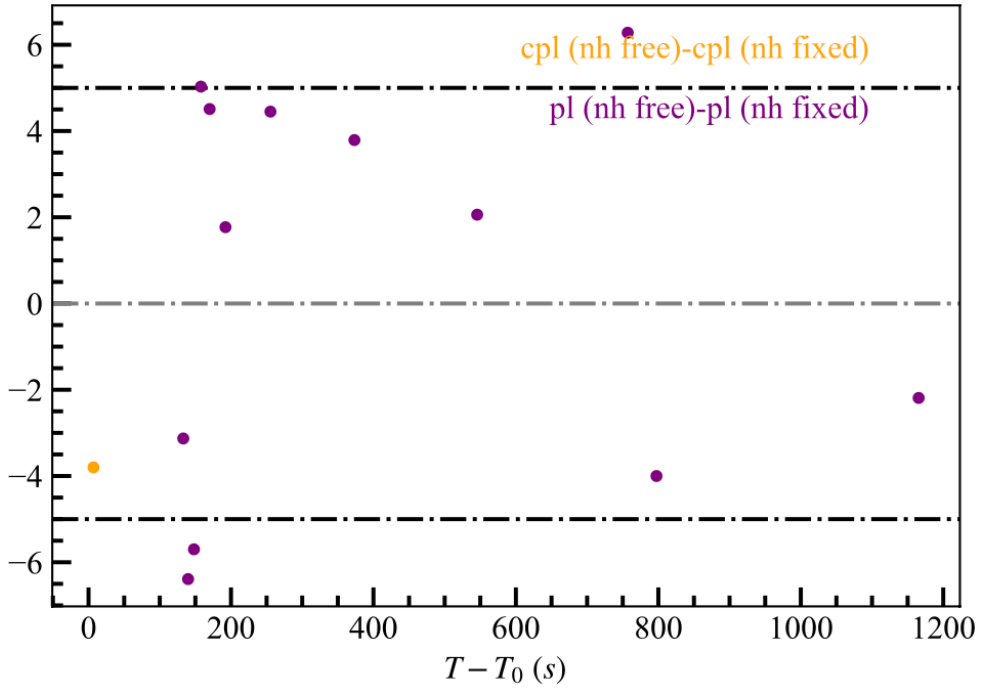

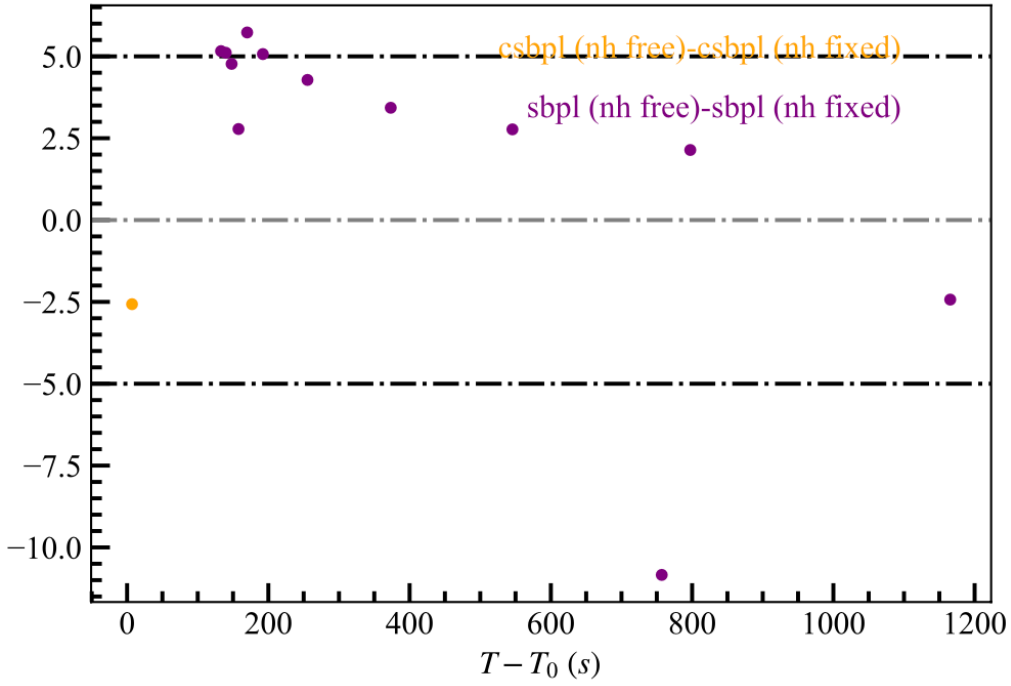

We fix $N_{H,int,1}$ at 3.73e22 cm^{-2} and $N_{H,int,2}$ at 6.39e21 cm^{-2} (best-fit from time-integrated spectrum) in light of:
1. time-dependent $N_{H,int}$ is expected because of photoionization and dust destruction*, and observed in the data
2. free $N_{H,int}$ in every time slice is not well constraint with large error bar
3. free or fixed intrinsic $N_{H,int}$ do not significantly affect spectral indices

The reduction of pile-up effect

The problem in afterglow SED

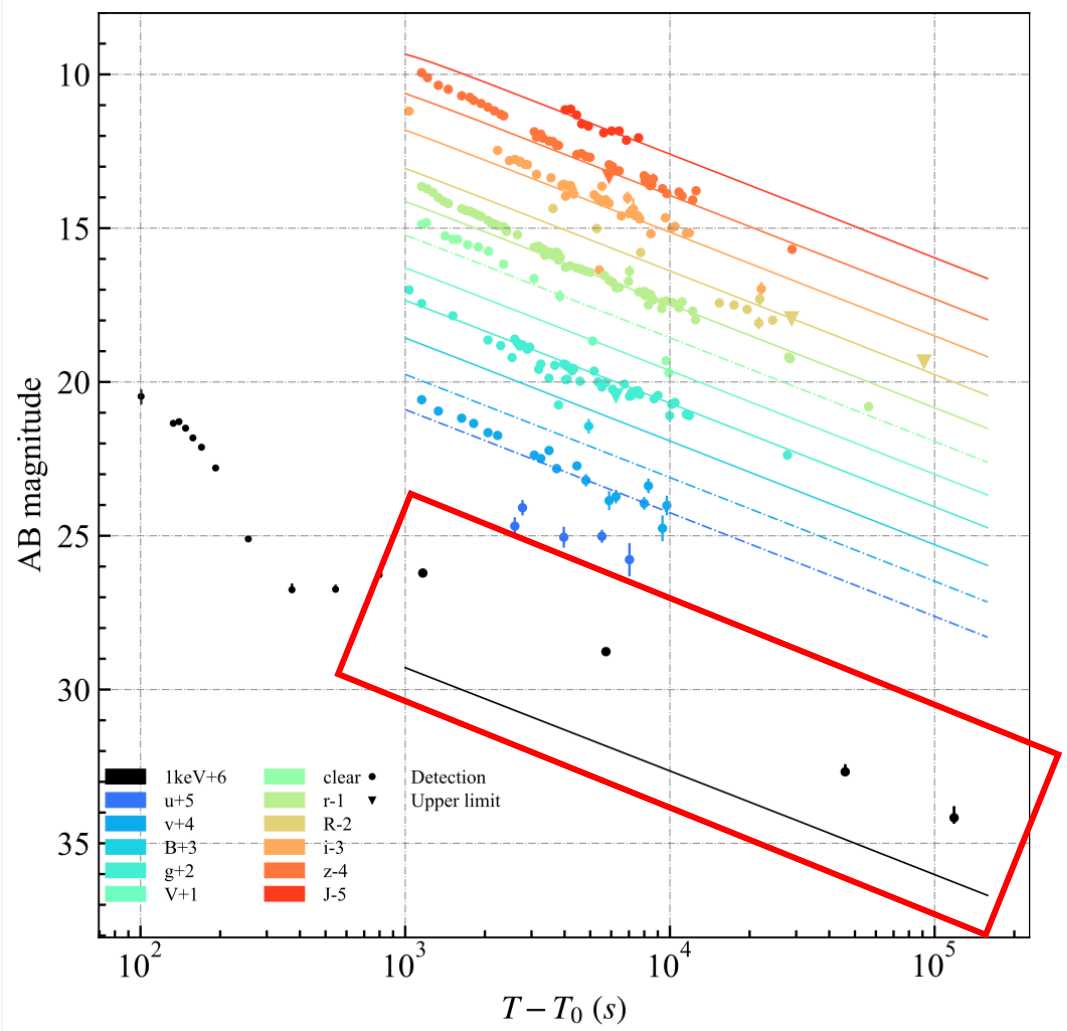

x-ray flux excess

The problem in afterglow SED

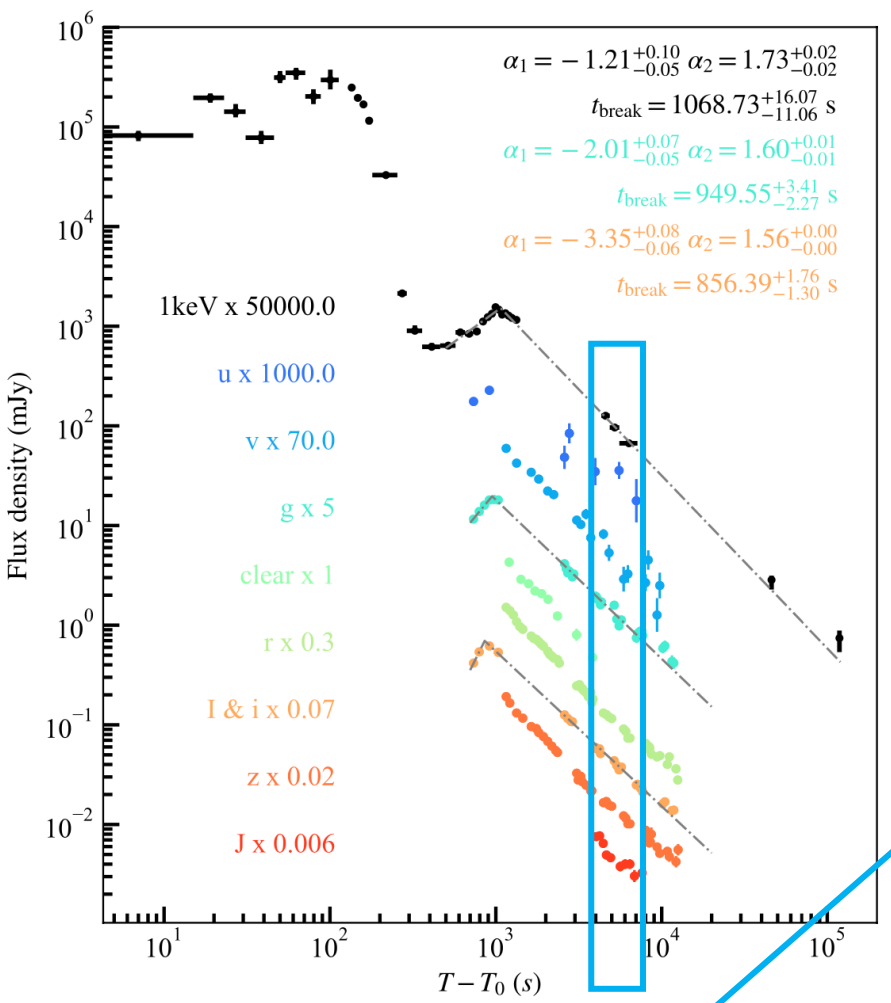

plot SED

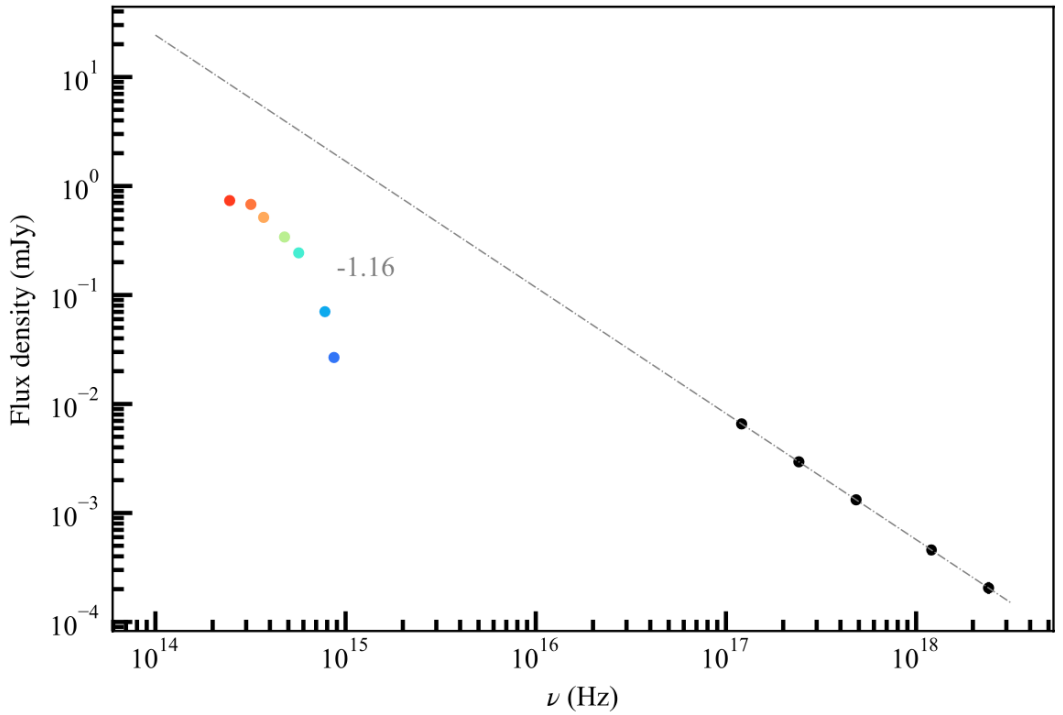

1. expecting a break, maybe ν_c
2. X-ray flux is overestimated

The problem in afterglow SED

FXT-A	shape centered on source
stage 1	annulus (45-85 arcsec)
stage 2	annulus (25-85 arcsec)
stage 3	circle (85 arcsec)
FXT-B	shape centered on source
stage 1	annulus (45-120 arcsec)
stage 2	annulus (20-120 arcsec)

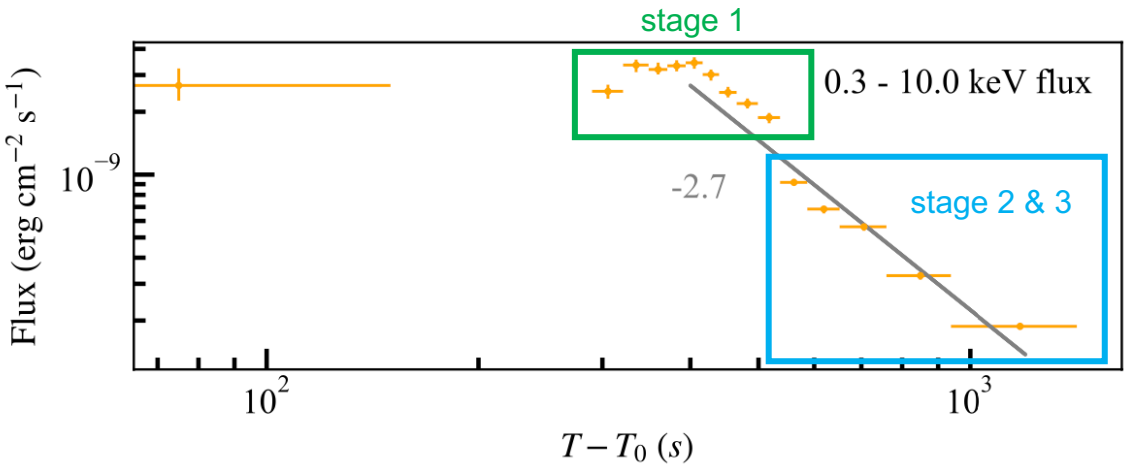

The problem with EP250304a:

PSF correction might be inaccurate!

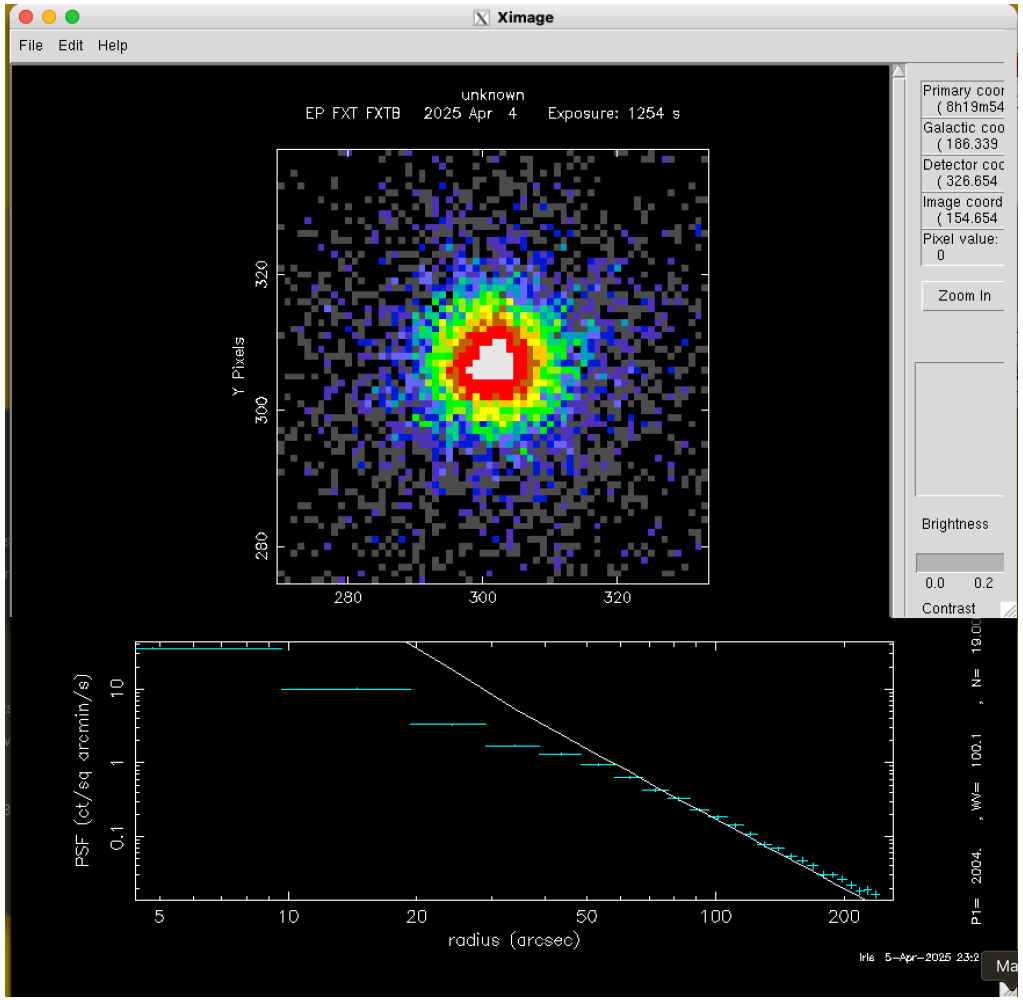

use 70-150 arcsec annulus region from 130-7143 s to avoid relative flux uncertainty

The problem with pile-up reduction: PSF correction is wrong

relatively right, absolutely wrong

Original:

FXT-A + FXT-B joint fit	const * tbabs * ztbabs * pl	70-150 arcsec	130-7143s
FXT-A + FXT-B joint fit	const * tbabs * ztbabs * pl	40 arcsec	44412-122326s

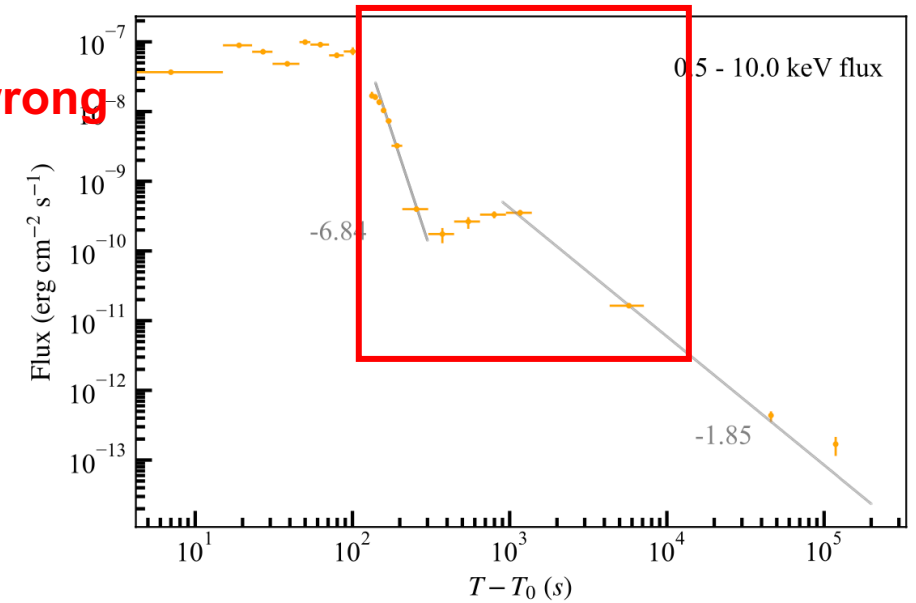

absolutely right, relatively wrong

Solution:

FXT-A fit	tbabs * ztbabs * pl	70-150 arcsec	130-255s
FXT-A fit	tbabs * ztbabs * pl	40 arcsec	255-7143s
FXT-A + FXT-B joint fit	const * tbabs * ztbabs * pl	40 arcsec	44412-122326s

(FXT-B ff mode is severely suffered from pile-up up to ~ 7000 s)

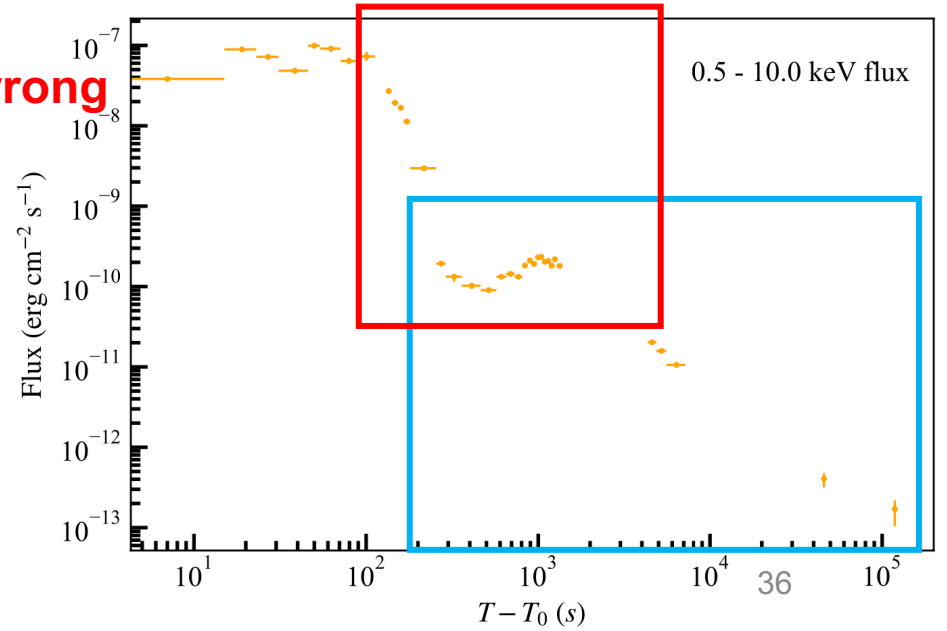

The effect of X-ray dust-scattering rings

FXT PSF

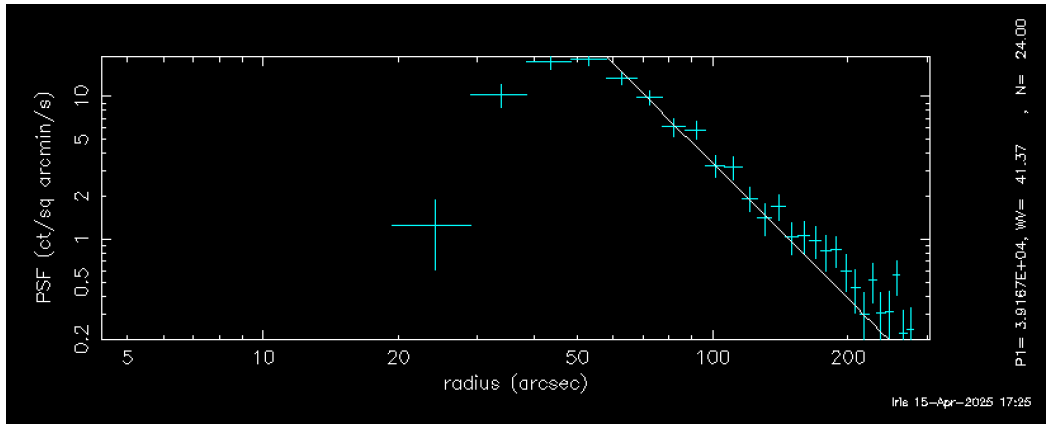

int00

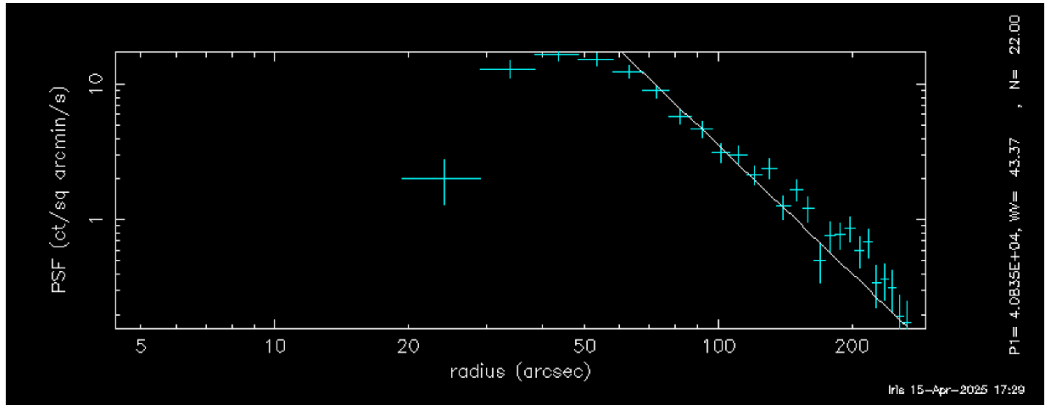

int01

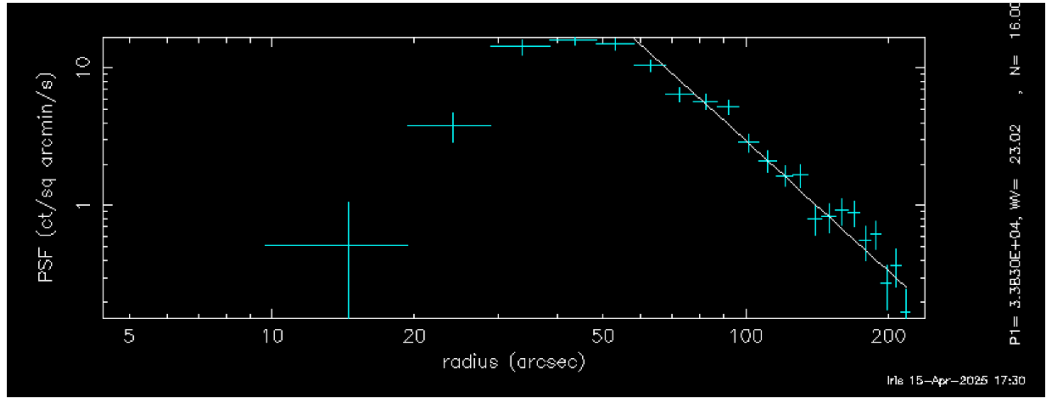

int02

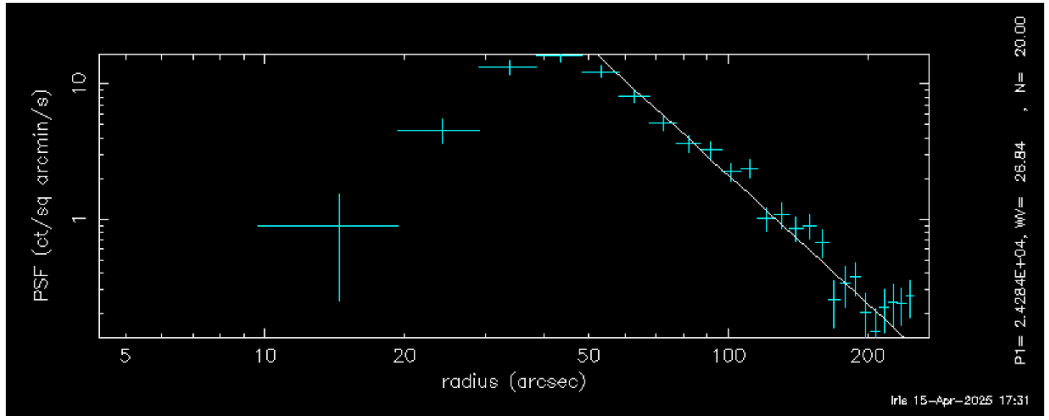

int03

FXT PSF

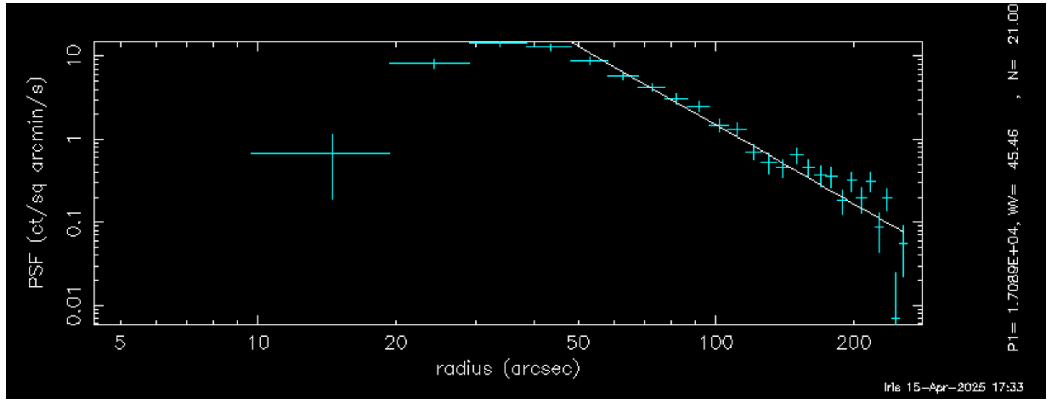

int04

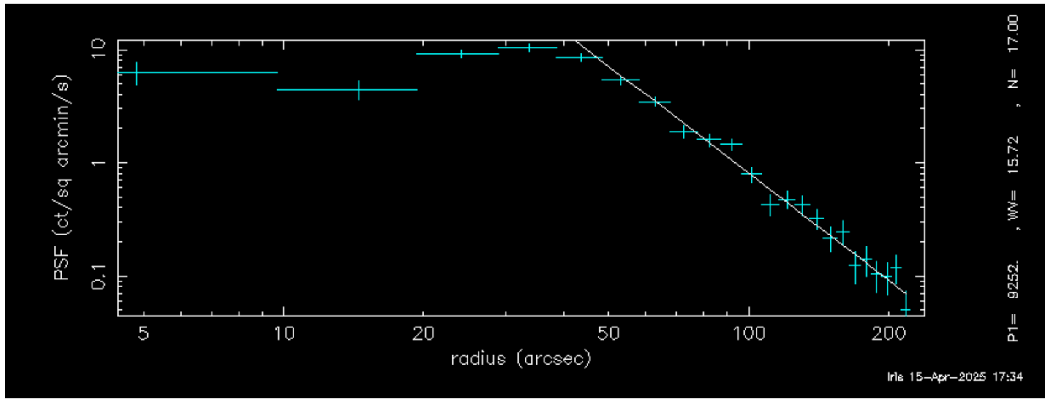

int05

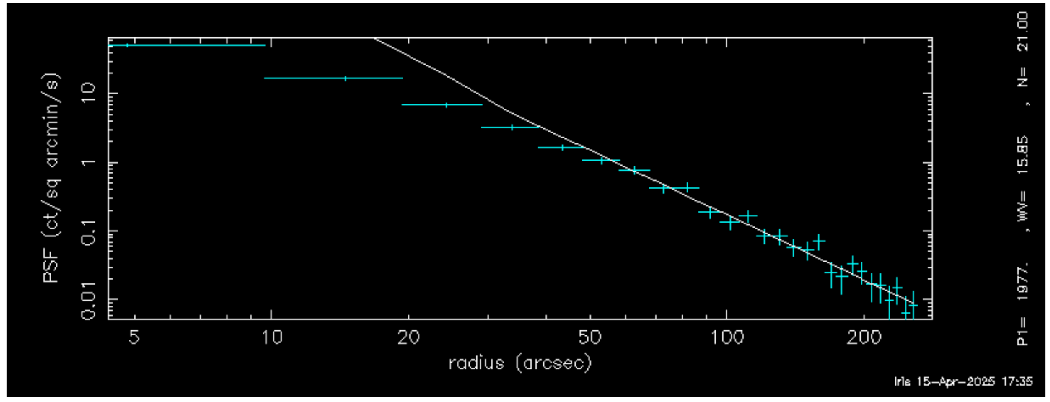

int06

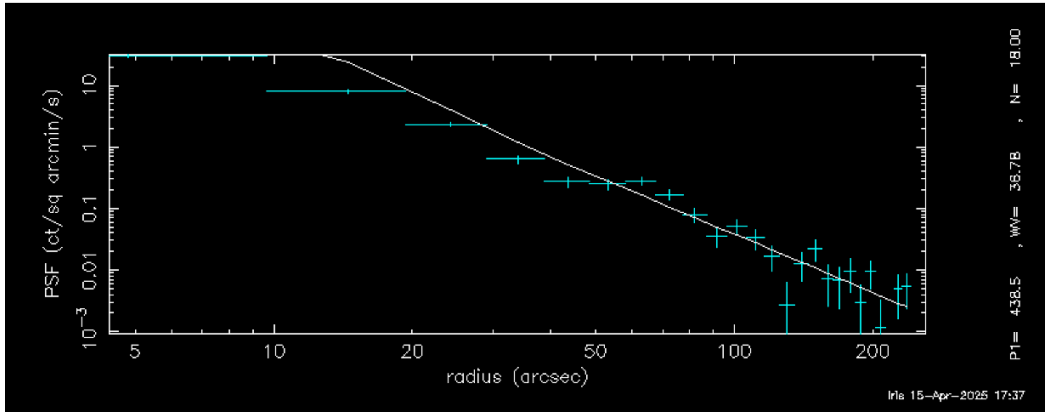

int07

FXT PSF

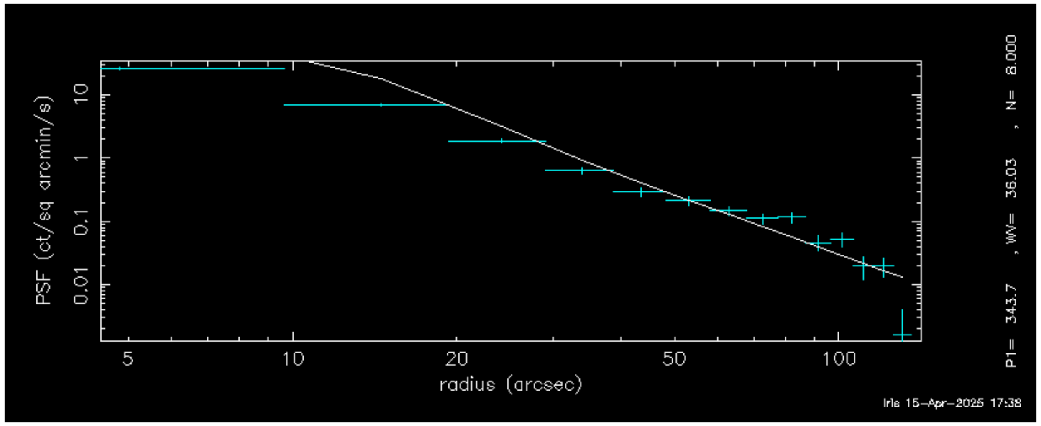

int08

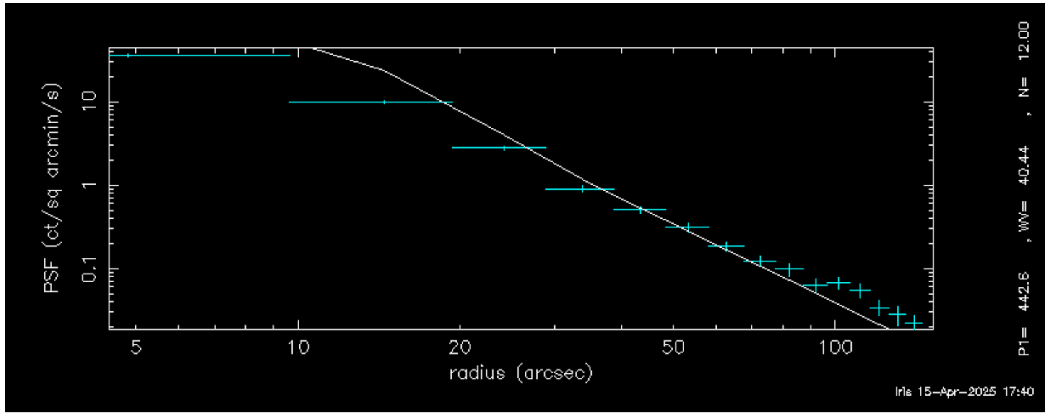

int09

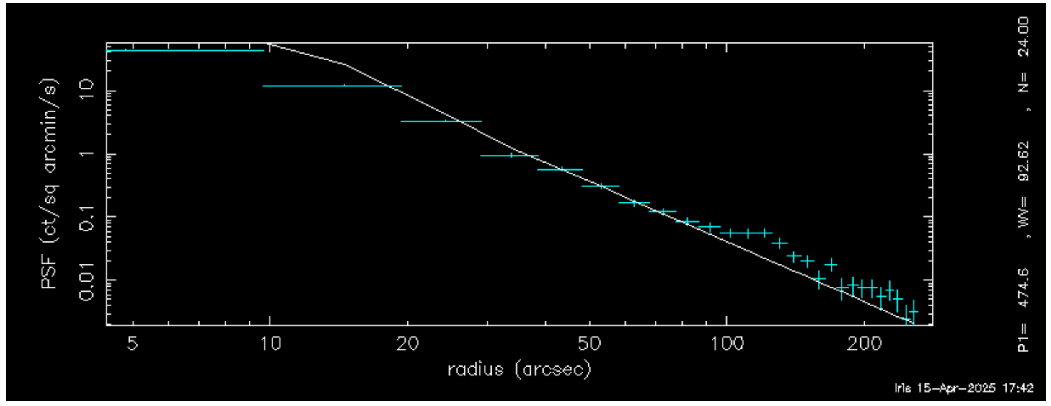

int10

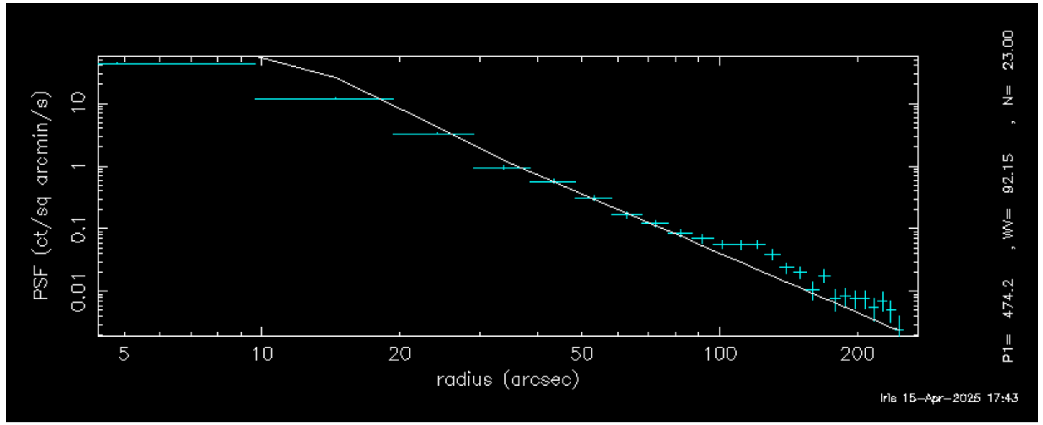

int11 (time-integrated)